CLONING AND STUDYING THE ROLE OF *MYCOBACTERIUM TUBERCULOSIS* MULTI-COPPER OXIDASE IN INHIBITING THE RESPIRATORY BURST

By

Ayat Kinkar

A thesis submitted in partial fulfillment

of the requirements for the degree of

Master of Science (MSc) in Biology

The Faculty of Graduate Studies

Laurentian University

Sudbury, Ontario, Canada

THESIS DEFENCE COMMITTEE/COMITÉ DE SOUTENANCE DE THÈSE
Laurentian Université/Université Laurentienne
Faculty of Graduate Studies/Faculté des études supérieures

Title of Thesis Titre de la thèse	CLONING AND STUDYING THE ROLE OF MYCOBACTERIUM TUBERCULOSIS MULTICOPPER OXIDASE IN INHIBITING THE RESPIRATORY BURST
Name of Candidate Nom du candidat	Kinkar, Ayat
Degree Diplôme	Master of Science
Department/Program Département/Programme	Biology
Date of Defence Date de la soutenance	October 20, 2016

APPROVED/APPROUVÉ

Thesis Examiners/Examinateurs de thèse:

Dr. Mazen Saleh
(Supervisor/Directeur(trice) de thèse)

Dr. Robert Lafrenie
(Committee member/Membre du comité)

Dr. Jeffrey Gagnon
(Committee member/Membre du comité)

Dr. Sreekumari Kurissery
(External Examiner/Examinateur externe)

Approved for the Faculty of Graduate Studies
Approuvé pour la Faculté des études supérieures
Dr. Shelley Watson
Madame Shelley Watson
Acting Dean, Faculty of Graduate Studies
Doyenne intérimaire, Faculté des études supérieures

ACCESSIBILITY CLAUSE AND PERMISSION TO USE

Abstract

Mycobacterium tuberculosis is the etiological agent of the pulmonary disease Tuberculosis. It affects more than one-third of the world's population. During bacterial infections, macrophages and other phagocytic cells of the immune system target and neutralize the causative agent. Following phagocytic uptake of bacteria by the macrophages, the phagolysosomal compartment produces reactive oxygen species (ROS) through the so-called respiratory burst to control the infection. Recent work by several groups indicates that pathogenic *M. tuberculosis* can survive phagocytic uptake by macrophages through inhibition of the respiratory burst. I have cloned and expressed Rv0846c, a protein known to be a membrane-associated multi-copper oxidase from *M. tuberculosis* (MmcO). I hypothesised that MmcO suppresses the production of ROS and may thus contribute to the survival of the pathogen during phagocytosis. Purified MmcO displayed a significant activity against the model substrate ABTS. Various amounts of active MmcO were tested against the ROS production in THP-1 monocyte cell line. Streptolysin-O-permeabilized THP-1 cells that were exposed to 500 ng of the purified MmcO protein displayed a significant reduction in the level of induced ROS by phorbol 12-myristate 13-acetate (PMA). This study indicates that the MmcO has a potential role as a virulence factor for *M. tuberculosis*.

Keywords: *M. tuberculosis*, Multi-copper oxidase, Reactive oxygen species, Phagocytosis.

Acknowledgments

This thesis is dedicated to my Father. For his support, unremitting encouragement, and endless love even on his deathbed God bless his soul.

It is an honor to extend my sincere thanks and gratitude to a number of people without whom this thesis might not have been completed and to whom I am greatly indebted.

First and foremost, I would like to sincerely thank my supervisor, Dr. Mazen Saleh for his guidance, support, and expertise were very beneficial throughout this study. His confidence in me made the completion of the present study possible. I would also like to thank Dr. Robert Lafrenie for being one of my thesis committee members as well as his generous assistance to perform some experiments in his lab. My gratitude is also extended to Dr. Jeffrey Gagnon, who is a committee member, for the discussion and the suggestions he provided at all levels of the project. A special thank goes to Dr. Pejman-Hanifi Moghaddam for being such a good mentor in my fourth-year thesis and for the knowledge and great skills you have imported on me. His influence towards my success today is highly acknowledged.

I would also like to express my gratefulness to Dr. Paul Michael for his time, suggestions, and advice during the research project.

To my family, especially my Mather and sisters, thank you for giving me the inspiration, support, and strength to reach the stars and chase my dreams. Very special and wholehearted thank goes to my brother, Eyad, who without his assistance and patience I would not be able to complete this project.

To all my friends especially Hanadi Alousaimi and Fatema thank you for the love, understanding, and encouragement when was needed. Their friendship makes my life unforgettable and wonderful experience.

Finally, I would like to thank the Ministry of High Education of Saudi Arabia for the financial support during this journey.

Table of Contents

List of Figures

List of Abbreviations

Amp	Ampere
ATP	Adenosine triphosphate
BCG	Bacille Calmette-Guerin
bp	Base pair
DMSO	Dimethyl sulfoxide
DTT	Dithiothreitol
EDTA	Ethylenediaminetetracetic acid
g	Gram
HEPES	4-c2-hydroxyethyl-1-piperazinethane sulfonic acid
HIV	Human immunodeficiency virus
h	Hour
IPTG	Isopropyl β-D-1-thiogalactopyranoside
kDa	Kilodalton
L	Liter
LB	Luria Bertani
M. tuberculosis	*Mycobacterium tuberculosis*
M. bovis	*Mycobacterium bovis*
M. smegmatis	*Mycobacterium smegmatis*
M	Molar
mM	Millimolar
µM	Micro molar
nM	Nano molar
mg	Milligram
µg	Microgram
ng	Nano gram
µm	Micrometer
nm	Nanometer

mL	Milliliter
μL	Microliter
min	Minute
MmcO	Mycobacteria multicopper oxidase (rv0845c)
MPC	Mycobacterium pathogen complex
NADPH	Nicotinamide Adenine Dinucleotide Phosphate Oxidase
NCBI	National Center for Biotechnology Information
OD	Optical density
PBST	Phosphate buffered saline with 0.1% Tween-20
PBS	Phosphate buffered saline
PCR	Polymerase chain reaction
PMA	Phorbol 12-myristate 13-acetate
RB	Respiratory burst
ROS	Reactive oxygen species
RP	Reverse primer
RPM	Revolutions per minute
RT	Room temperature
SDS-PAGE	Sodium dodecyl sulfate polyacrylamide gel electrophoresis
SLO	Streptolycin O
TAE	Tris acetate EDTA buffer
TB	Tuberculosis
TEMED	Tetramethylethylenediamine
U	Unit
UV	Ultraviolet
V	Volt
v/v	Volume per volume
w/v	Weight per volume
xg	Times gravity

Introduction

Mycobacterium tuberculosis as a public health threat

Mycobacterium tuberculosis (*M. tuberculosis*) is widely recognized as the etiological agent of the pulmonary disease Tuberculosis in humans. *M. tuberculosis* belongs to the Mycobacteriaceae family that consists of 150 species under a single genus being Mycobacterium (Lory, 2014). It is possible for a species of Mycobacteriaceae to be present in water and soil, from where they can establish their presence in animals and humans causing disease (Galagan, 2014; Deffert, 2014). A number of species are pathogenic and slowly growing mycobacteria that have a doubling time of 24h such as *M. tuberculosis*. Other species are non-pathogenic and fast-growing mycobacteria which can multiply every 3-4 h including *Mycobacterium smigmatis* (Klann et al, 1998). Despite the fact that Mycobacteriaceae's species are taxonomically different (pathogen and non-pathogen), the main characteristics of the cell wall shared by all these species are almost identical.

The Mycobacteriaceae family is catagorized as being acid-fast, aerobic, as well as non-spore forming bacilli (Sakamoto, 2012). The outstanding trait of this family is the unique waxy cell wall. The waxy cell wall contains lipids, peptidoglycan layers and hydrophobic mycolic acids, which is anchored by arabinogalactan (Figure1) (Hett & Rubin, 2008). Mycolic acid is a wax coating representing approximately 50% of the dry weight of the cell wall. This is what renders the cell wall impermeable to a number of chemicals included in the gram stain (Kleinnijenhuis et al, 2011). The only effective stain for Mycobacteriaceae is the Zhiel-Neelson stain, which is an acid-fast pigmentation stain. Nevertheless, researchers have classified the Mycobacteriaceae family members as Gram- positive organisms based on genetic similarities.

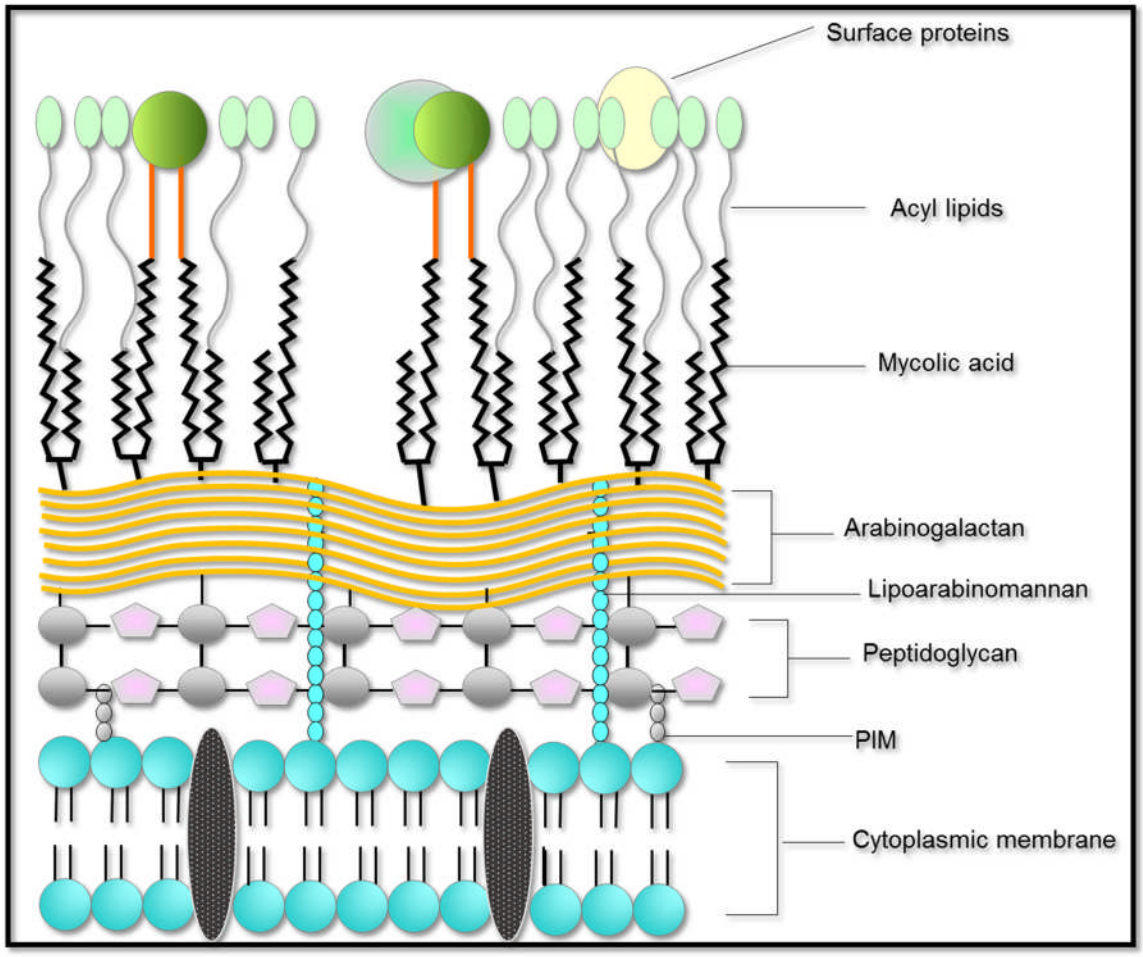

Figure 1: The structure of the Mycobacterial waxy cell wall. This Figure demonstrates the main components of the cell wall and their distribution. Above the cytoplasmic bilayer membrane, the inner layer is comprised of peptidoglycan that links to arabinogalactan layer covalently and lipoarabinomannan is elongated between both of them. The outer membrane is made of mycolic acids, and outer lipids layer along with surface protein. This Figure is adapted from http://faculty.ccbcmd.edu/courses/bio141/lecguide/unit1/prostruct/u1fig11.html

Furthermore, the pathogenic members of this family are grouped under the Mycobacterium Pathogen Complex (MPC) group (Forrellad et al, 2013; Lory, 2014). A number of species make up the MPC that includes *M. tuberculosis, Mycobacterium africanum*, *Mycobacterium bovis*, *Mycobacterium canettii*, *Mycobacterium microti*, *Mycobacterium caprae* and *Mycobacterium pinnipedii*. Studies have demonstrated similarities among these species at the genomic level (Forrellad et al, 2013). The *M. tuberculosis* genomic DNA, for example, has a 99.95% sequence identical with the *M. bovis* DNA sequence (Sakamoto, 2012). Research has shown that *M. tuberculosis* is characterized as a non-motile, non-sporulating acid-fast bacillus. Although *M. tuberculosis* is classified as Gram-positive according to the genomic similarity (phylogenetic analysis) and the thick peptidoglycan (PG) or murein layer (Sakamoto, 2012), it is structurally related to Gram-negative bacteria. This similarity is a result of having similar cell wall components, pseudo-periplasm, and pseudo-outer-membrane (Hett & Rubin, 2008; Fu & Fu-Liu, 2002). Therefore, classifying this bacterium as one of either Gram stains has not been determined. *M. tuberculosis* requires an aerobic oxygenated environment in order to multiply. It multiplies in a slow manner due to slow passing of nutrients through the cell wall. This feature makes it possible for *M. tuberculosis* to develop and become resistant to recognition by the host immune system (Kleinnijenhuis et al, 2011).

Epidemiological studies demonstrate that *M. tuberculosis* H37Rv is a prevalent virulent strain that causes TB. Its genome is made up of 3,925 identified genes and ~250 genes out of this total participate in fatty acid metabolism during the dormant period within the host cell (Cole et al, 1998). In North America and Europe, major epidemics broke out during the 18^{th} and the 19^{th} centuries but *M. tuberculosis* was identified as the etiological agent of TB in 1882 by Robert Koch (Sakamoto, 2012; Comas et al, 2013). It was proposed, based on recent studies on the bacterium

genome sequences, the emergence of *M. tuberculosis* took place in Africa approximately 70,000 years ago (Comas et al, 2013; Cambier et al, 2014). Since then *M. tuberculosis* bacilli have evolved and been transmitted worldwide from one infected person to another causing TB infection (Daniel, 2006; Galagan, 2014). Data from the World Health Organisation (WHO) indicates that approximately one-third of the global population is infected with *M. tuberculosis* and out of this number, 1.5 million people lose their lives as a result of TB. In fact, it is estimated that 1 of 3 deaths in people who are HIV-positive are contributed to TB (WHO Tuberculosis Fact Sheet N104, 2016). The prevalence of TB varies by region: in the U.S.A, for example, there were 2.96 cases of TB per 100 000 people in 2014. Among people migrating to the US, the rate of infection is higher, by a factor of 13, compared to people who were born in the US (WHO Global Tuberculosis Report 2014).

Tuberculosis infection

M. tuberculosis can be described as an aerobic bacterium, which mostly affects the lungs. Other parts of the body, such as the lymphatic and central nervous as well as the gastrointestinal and circulatory systems can also be affected by *M. tuberculosis* (Dwivedi, 2011). *M. tuberculosis* transmission occurs through the inhalation of aerosolized droplets coming from the coughing or sneezing of an infected person. After inhalation, the pathogen is phagocytosed by the lung's alveolar macrophages (Shi & Darwin, 2015). In some cases, the pathogen can possibly escape the macrophage's phagocytosis process in order to multiply and disrupt the macrophage. This disruption allows the pathogen to be ingested by blood-derived macrophages that were initially recruited by the release of the chemokines. In this stage of infection, the blood- derived inactive macrophages create an environment for the pathogen to start a logarithmic growth but not to

eliminate it (Kleinnijenhuis et al, 2011). Approximately 2 to 3 weeks after infection has established itself in the early lesions, the T lymphocytes multiply and the T helper (T_H) cells signal for the release of pro-inflammatory cytokines including interferon-γ (IFNγ) to activate macrophages and promote the destruction of the intracellular *M. tuberculosis*. Consequently, the intracellular growth of the pathogen ceases and extracellular pathogen growth becomes restricted within the central solid Caseous necrosis that is present in the early lesions or granulomas. The purpose of this Caseous necrotic tissue in the granuloma is to control the pathogen spread and to protect the lungs from becoming damaged (Kleinnijenhuis et al, 2011).

When an infection remains dormant within a granuloma, it is referred to as a latent TB infection. It may take months or years before reactivation can take place, or reactivation may even fail to take place in an individual with a healthy immune system. The reactivation of the bacterium generally occurs under a failure in immune surveillance. This can occur when the host is exposed to co-infections with HIV or with certain factors like old age, or during treatment with medications that result in an immunosuppressive state (Smith, 2003; Boshoff & Barry, 2005; Verver et al, 2005). Latent TB can then become reactive and is known as active TB. Active TB leads to death only if the patients with immune system failure are suffering from other diseases including malignancy, liver cirrhosis, renal failure, and pneumonia (Lin et al, 2014). The weakness of the body's immune system promotes *M. tuberculosis* to multiply and attack the lung or other parts of the body via the bloodstream. In another word, the *M. tuberculosis* defeats the immune system responses. Patients with active TB are more likely to die due to Septic shock as well (Lin et al, 2014). TB also is considered as a cause of respiratory failure called acute respiratory distress syndrome (ARDS). ARDS leads to death when the lung inflammation, hypoxemia and frequently multiple organ failures are caused by the reduction in gas exchange and the systemic release of

inflammatory mediators (Raina et al, 2013). Other than the disease, active TB can lead to death in cooperation with environmental factors, such as poverty and unhealthy diet (WHO Fact sheet N°104, 2016). As a result, TB leads to death only in the presence of cofactor diseases or environmental influence.

So far, only one vaccine has been approved to prevent TB infection and is known as the Bacille Calmette-Guérin (BCG) vaccine. BCG is an attenuated strain of *M. bovis* and since *M. bovis* causes TB in cattle and shares a 99.95% sequence similarity with the *M. tuberculosis* DNA sequence (Sakamoto, 2012), the genomic similarity makes it the perfect vaccine against human TB. However, it is effective in children, but not adults (Niki et al, 2015; WHO, 2015). This leaves antibiotics to be the only option for the treatment of TB infections. Active TB patients have both systemic and lower respiratory track symptoms including fever, night sweat, weight loss, vomiting, coughing up blood, chest pain, and belaboured breathing. Any patient in this situation requires intensive therapeutic treatment (CDC:Tuberculosis (TB) Disease: symptoms & Risk Factors, 2016).

Treatment of active Tuberculosis

To many scientists, the treatment of this disease has become a global challenge in their attempt to prevent disability and death, as well as in halting the spread of the disease. Several effective drugs have been developed over the years for treating patients suffering from active TB infection. TB drugs, unlike those for many other infectious diseases, are given for a long period of time. Additionally, the use of a single antibiotic for the treatment of TB infection is proving to be ineffective. Streptomycin, the first successful antibiotic to be used against TB, provided the first case in the history of resistance to a drug during the treatment for TB infections, in 1940s

(Keshavjee & Farmer, 2012). In 1943, Salvador Luria and Max Delbruck came up with a demonstration to prove that random genetic mutation occurred even when there was no selection pressure by antibiotics (Murray, 2016). Thus, it became important to note that resistance to the drugs always developed when a signal drug was used for treatment but the resistance was much lower when a combination of at least two drugs were used for treatment (Keshavjee & Farmer, 2012). It was also believed, *M. tuberculosis* morphology also contributed to drug resistance in that it has a waxy cell wall, which enhances resistance to antibiotics, acidity, and alkalinity (Daffe & Draper, 1998).

Current treatment for TB requires a multiple drug regimen. Upon confirmation of disease, a combination of up to four antibiotics, known as RIPE, are used as the initial course of drug treatment. These drugs are rifampin (RIF), isoniazid (INH), pyrazinamide (PZA), and ethambutol (EMB). The course of intensive treatment is strictly for a period of two months to ensure that the pathogen is completely eradicated. The patient can then be placed on a less aggressive treatment with only RIF and INH for an additional 4 months (CDC "Treatment for TB_Disease", 2016). As a result of patients missing doses or stop to complete the treatment courses, *M. tuberculosis* increases its immune resistance and expresses enzymes. These enzymes combat the action of the available drugs (Forrellad et al, 2013), and lead to the development of the multidrug resistance strains. That means the therapy frequently will last from six months to two years to minimise resistance. However, the WHO data showed that the multidrug resistance strains of *M. tuberculosis* have emerged from 3.3% of new cases and up to 20% of treated cases as a side effect of prolonged antibiotic therapy (WHO Global Tuberculosis Report 2015). *M. tuberculosis* has developed multidrug resistance strains. Therefore, a comprehensive understanding and characterizing the

interaction between the immune system of the host and the pathogen would lead to new therapeutic strategies.

Pathogen-host interactions in TB

M. tuberculosis can develop resistance to the immune system of the host in addition to treatment strategies, which has made its eradication difficult. Despite the fact that no classical virulence factors such as toxins are existed in *M. tuberculosis* (Forrellad et al, 2013), *M. tuberculosis* can effectively cause infection and survive within the host for a very long period (Sakamot, 2012). Thus, *M. tuberculosis* is unique as compared to other microorganisms, because its persistence inside the host is due to its transmission cycle and its ability to compromise the human immune system (Prozorov et al, 2014; Cambier et al, 2014).

During pathogenic infections (non-TB), the immune system recognises the bacteria as invading pathogen. Activation of the innate immune system involves the process called phagocytosis by the macrophages or neutrophils. The phagocytosis process starts by an engulfing stage, when the macrophages are activated by the pathogen through stimulation of the Pattern Recognition Receptors (PRRs) such as cytokines IFN- γ, Toll-like receptor 2 (TLR2), or other phagocytic receptors (Weiss & Schaible, 2015). After that, the engulfing stage of the pathogen into a phagosomal vacuole within the macrophages, where the pH is about 6.4. This stage forms the early phagosome and leads to the production of more anti-microbial reactions (Weiss & Schaible, 2015; Tan & Russell, 2015). The early phagosome stage is marked by small GTPase markers including Rab5A (Weiss & Schaible, 2015). Then the maturation stage is when the membrane of the phagosome fuses with the lysosome in the presence of phosphatidylinositol 3-phosphate (PI3P), and generating the phagolysosome. PI3P is a phospholipid found in cell membranes as it

is synthesized by a phosphatidylinositide 3 kinase (Weiss & Schaible, 2015). The phagolysosome stage is marked by the interchange between Rab7A and Rab5A on the phagolysosome membrane (Weiss & Schaible, 2015). This stage introduces the slow reduction of the pH inside the phagolysosome compartment by activation of the ATP-dependent proton pumps (Sturqill-Koszycki et al, 1994; Deffert et al, 2014) to destroy the pathogen through acidification (pH 4.5). The acidification results in the activation of the hydrolytic enzymes (Figure 2) (Deffert et al, 2014) and the stimulation of the NADPH oxidase to generate Reactive Oxygen Species (ROS), which consequently causes the respiratory burst against the pathogen. Although phagocytosis is an effective process to eradicate most pathogens, there are several pathogens like *Listeria* and *Shigella* that escape the phagocytosis process and reproduce in the cytoplasm (Smith, 2003). Other bacteria, like *Salmonella typhimurium*, not only can survive the phagocytosis process but also require the acidic environment of the macrophage phagolysosome such as pH 4.6 in order to survive (Rathman et al, 1996).

It is a different case when it comes to *M. tuberculosis* infection. *M. tuberculosis* has a more complex cycle in the macrophage and requires blocking of phagosomal maturation, lysosome fusion, and the prevention of acidification of the phagosome environment which allows the pathogen to escape destruction and live in macrophages. Similar to all pathogenic infection, the host innate immune system recognises the *M. tuberculosis* via different receptors. These different receptors of macrophage interact with *M. tuberculosis* to generate various responses (Figure 2). *M. tuberculosis* interacts with TLR2 by pathogen-components like phosphatidylinositol mannosidase (PIMs) and lipoarabinomannan (LAM) on its surface and promotes inflammation (Sakamoto, 2012). *M. tuberculosis* has the ability to utilise some of the macrophage receptors for its benefit, for example, *M. tuberculosis* engages to the mannose receptor (MR) or complement

receptor 3(CR3) to evade the respiratory burst and phagosome maturation (Armstrong & Hart, 1975; Kang et al, 2005). After the pathogen recognition step, the macrophage phagocytosis process stops at the early phagosome where the *M. tuberculosis* is able to resist and slowly proliferate. This happens due to the *M. tuberculosis* ability to adapt to the harsh condition of the host environment and to defend its self from the antibacterial action of the phagosome. *M. tuberculosis* adaptation strategy is ascribed to its fatty acids usage as a substitute metabolic component for glucose. This leads to thickening its cell wall and making it impermeable. In addition to the *M. tuberculosis's* ability to adapt to the environment of the host cells, *M. tuberculosis* virulence factors is essential for its defence strategies. Firstly, Lipids in the form of Phthiocerol Dimycocerosate (PDIM) protect the cell wall from detection by macrophages PRRs. Research has shown that lipid phosphatase production and secreted acid phosphatase SapM, through PI3P hydrolysis, prevent the fusion of the phagosome with the lysosome. *M. tuberculosis* contains surface lipids and LAM, as well as cord factor which impedes vesicle fusion (Pethe et al, 2004). Secondly, Tryptophan Aspartate Coat Protein (TACO) constraints phagosome-lysosome fusion through the activation of calcium-dependent phosphatase calcineurin (Figure 2) (Sakamoto, 2012; Weiss & Schaible, 2015). Finally, the degradation of the pathogen by macrophages through phagosome acidification is prevented by *M. tuberculosis* induced depletion of the level of the phagosome proton-ATPase making the acidification ineffective and resulting in *M. tuberculosis* survival at a pH of approximately 6.5 (Sturqill-Koszycki et al, 1994; Weiss & Schaible, 2015). Remarkably, the interaction of *M. tuberculosis* with lipid compartment bodies or droplets of lipid within the macrophage ensures a continuous source of nutrient for *M. tuberculosis*. The whole process of *M. tuberculosis* phagocytosis can be characterized as an early phagosome stage associated with Rab5A (Weiss & Schaible, 2015).

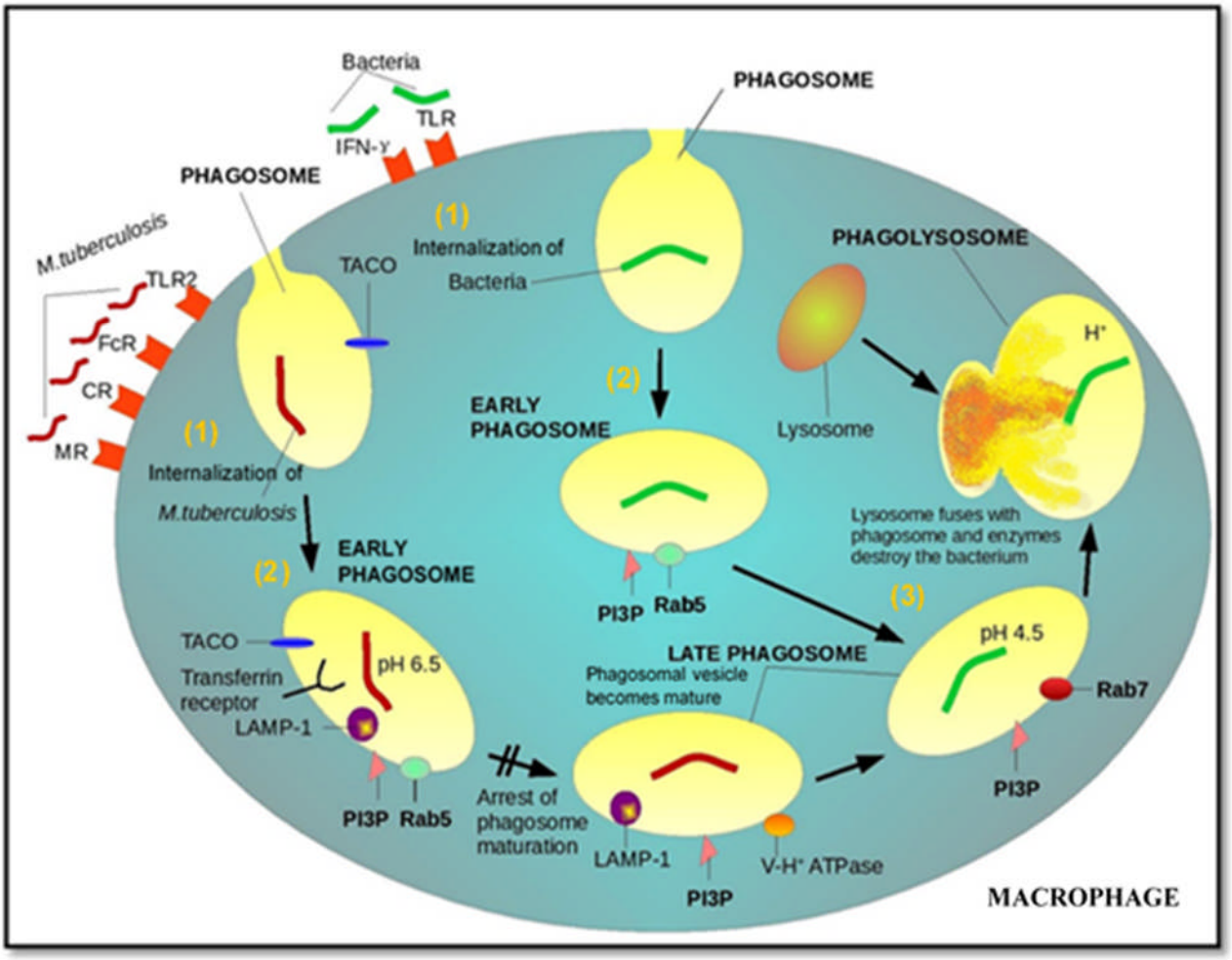

Figure 2: Phagocytosis in macrophages: the Figure shows the internalization and degradation of microbes under normal condition and in case of the infection with *M. tuberculosis* where the maturation processes are interrupted. The Figure is adapted from (Kaufmann, 2001).

Mechanisms for elimination and control of the pathogen by phagocytic cells – Respiratory Burst

To eliminate and control the threat of pathogens, host cells employ a variety of mechanisms including granuloma formation, phagolysosome fusion and even apoptosis to prevent pathogen replication. However, the macrophages' antimicrobial activity is largely defined by respiratory or oxidative bursts. The respiratory burst (RB) describes the process when reactive oxygen species (ROS) are rapidly released to terminate the targeted bacteria (Seres et al, 2000; Smith, 2003). ROS can be generated by the activation of Nicotinamide Adenine Dinucleotide Phosphate Oxidase (NADPH) during the last stages of phagocytosis. NADPH oxidase is a membrane-associated enzyme that is composed of five subunits which are NOX2 (gp91phox), p67phox, p22phox, p40phox, and p47phox. The key electron transporter is Gp91phox (Figure 3).

The RB starts when the NADPH subunits assemble into a complex that is enzymatically active causing the reduction of the O_2 molecule into superoxide anions (O_2-). The resulting electrons from the reduction reaction are transported through the cytochrome b to the oxygen molecules contained in the phagosome. Cytochrome b is a constitutive membrane protein present in phagosomes as well as the plasma membrane (Berton et al, 1986; Dahlgren & Karlsson,1999; Cross & Segal, 2004). The superoxide anions then dismutase into hydrogen peroxide (H_2O_2). Finally, H_2O_2 can combine with Cl^- in the presence of myeloperoxidase to produce Hypochlorous acid (Figure 4) (Kettle & Winterbourn, 1990) or can reduce copper or iron ions, resulting in hydroxyl radical (OH•) production. The cellular damage that includes damaged DNA and oxidation of lipid/protein is caused by Hypochlorous acid and hydroxyl radicals and eventually result in the destruction of the bacteria (Figure 4) (Kettle & Winterbourn, 1990; Poyart et al, 2001). The interaction of H_2O_2 with nitric radicals, to produce peroxynitrite ($ONOO^-$) and also contributes

to pathogen destruction (Ehrt & Schnappinger, 2009). ROS, besides being part of antimicrobial activities, plays a part in regulating cellular responses including apoptosis, cytokine release, and cell proliferation.

In spite of these effective anti-microbial activities, *M. tuberculosis* has adapted to grow inside macrophages. *M. tuberculosis* DNA is protected from oxidation by the use of histone-like proteins (LSR2) as a physical barrier and the presence of the UvrB endonuclease enzyme that works in repairing mycobacterial DNA (Saviola, 2013). The repair of *M. tuberculosis* oxidized proteins is handled through the activity of methionine sulfoxide reductase (Mst) (Deffert et al, 2014). *M. tuberculosis* also produces some enzymes that detoxify ROS (Ehrt & Schnappinger, 2009). Such as two superoxide dismutases (SodC and SodA), a catalase-peroxidase (KatG), mycothiol, NADH-dependent peroxidase, and peroxynitrite reductase (Deffert et al, 2014). Superoxide dismutase (SOD) is known for being a dynamic superoxide radical scavenger that can interfere with the production of ROS through the conversion of toxic superoxide to oxygen molecules and hydrogen peroxide (Liao et al, 2013). The study undertaken by Liao and his colleagues showed that purified SodA and SodC can inhibit respiratory burst free radical production (Liao et al, 2013). In addition, the hydrogen peroxide radical is converted into water by Catalase-peroxidase (KatG) (Ng et al, 2004; Mo et al, 2004). Since M. *tuberculosis* possesses the *rv0846c* gene that codes for the multi-copper oxidase (MmcO) with oxidoreductase ability, *M. tuberculosis* MmcO is a considerable candidate to inhibit reactive oxygen species (ROS) generation.

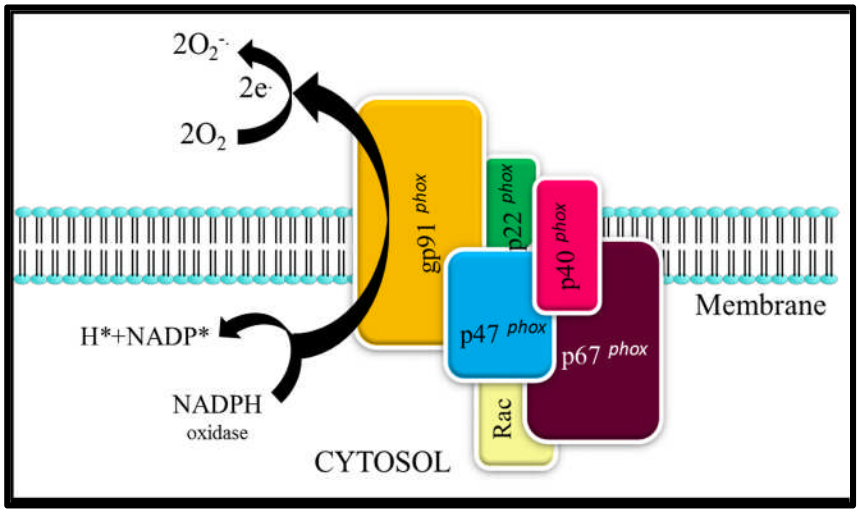

Figure 3: NADPH oxidase complex: the Figure represents the five subunits of NADPH complex, tow transmembrane units' gp91 and p22 that catalyze the transfer of electrons from cytosolic NADPH to molecular oxygen in order to generate the superoxide. The other subunits p47, p40, p67 work as regulator along with small GTPase Rac. This Figure is adapted from https://www.researchgate.net/Figure/257075489_fig1_NADPH-oxidase-structure-NADPH-oxidase-is-a-multi-subunit-enzyme-complex-present-in-the

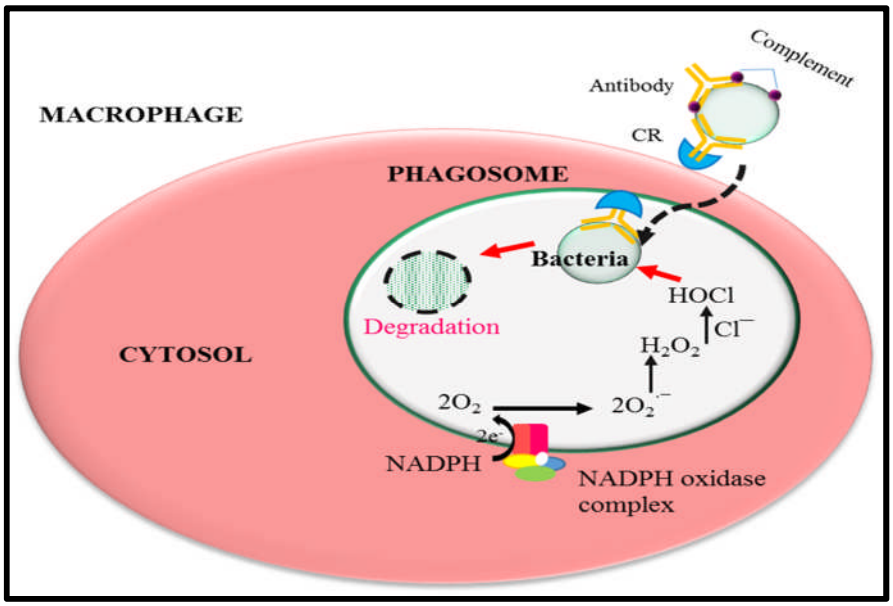

Figure 4: Macrophage respiratory burst: the Figure illustrates the process by which the macrophage NADPH oxidase generating the ROS to eradicate the pathogenic bacteria. This Figure is adapted from http://www.clinsci.org/content/111/1/1

Copper

Copper is an essential component and a functional co-factor for the MmcO enzyme. It also has been proven to be an essential cofactor for a range of enzymes including amine oxidases, which play a part in the generation of neurotransmitters; methane monooxygenases used by methanotrophs in the generation of energy; and SOD responsible for protecting cells against oxidative stress (Balasubramanian & Rosenzweig, 2007; Grass et al, 2011; Linder & Hazegh-Azam, 1996; Pena et al, 1999). At least two enzymes present in *M. tuberculosis* are known to require copper in their activities. Cytochrome c oxidase, which is the first enzyme, require copper as the terminal electron acceptor for aerobic growth (Shi et al, 2005). The second enzyme is superoxide dismutase (SodC) which copper and zinc are essential minerals for its activity to inhibit the oxidative burst of host macrophages (Piddington et al, 2001). Not only does cooper work as a co-factor for a number of enzymes, it also has roles in the energy generation and in the reduction of oxidative radical which make it an important element for cellular viability. In general, copper's importance to organisms is a result of its redox potential (Pena et al, 1999). In biological systems, copper possesses the ability to cycle between the toxic Cu1 and less toxic Cu2 states (Crichton & Pierre, 2001).

Copper Toxicity

In the innate immune response, copper is essential. Studies have demonstrated that mobilisation of essential metals like copper is a macrophages' way of increasing bactericidal activities. Macrophages increase the copper's toxicity in the phagosomal compartment by the accumulation of copper (Wagner et al, 2005) to promote the killing of bacteria. The respective rise in cellular copper and phagosomal copper are mediated by the copper transporters CTR1 and

ATP7A. Normally, when macrophages are exposed to lipopolysaccharide or interferon-γ activation, they increase the expression of both *atp7a* and *ctr1* (White et al, 2009). However, bacteria utilise different methods to fight against the high level of copper toxicity, by reducing the ATP7A protein levels to survive the copper presence within the phagosome (Wagner et al, 2005; White et al, 2009). As a result, there must be maintenance of the correct balance of copper needed as co-factor function while damage resulting from highly redox active metal is minimised.

MmcO, which consists four copper atoms, is initially introduced as a copper resistant enzyme for many identified bacteria including *Pseudomonas syringae* (Cha & Cooksey, 1991), *Salmonella enterica* (Achard et al, 2010), and *Escherichia coli* (Grass & Rensing, 2001). Several MmcOs have been found in other organisms, like fungi and other bacteria, together with human ceruloplasmin and plant ascorbate oxidase (Solomon et al, 1996; Quintanar et al, 2007). Interestingly, the structural morphology is almost similar in all discovered MmcOs. The involvement of bacterial MmcOs in copper resistance is through the detoxification of toxic copper Cu1 to less toxic Cu2 within the host's cells. Also, MmcO is needed for the purposes of virulence in bacteria like *Xanthomonas campertris* (Hsiao et al, 2011) and *Salmonella* (Achard et al, 2010). Research has demonstrated that the *M. tuberculosis* susceptibility to macrophage toxic copper has been increased by the knockout of *M. tuberculosis'* MmcO at least 10-fold; therefore, *M. tuberculosis* employs copper toxicity resistance which is facilitated by MmcO (Rowland & Niederweis, 2013). To sum up, MmcO has oxidative ability to block the copper toxicity by detoxification Cu1, this property could also employ the neutralizing/suppression of the ROS during respiratory burst since there is no study has been conducted yet on this concept.

Multi-Copper Oxidase (MmcO)

MmcO is a membrane-associated protein of *M. tuberculosis* with oxidoreductase activity. The *rv0846c* gene codes for MmcO, a 54 kDa protein that contains 504 amino acids. The *rv0846c* gene is well conserved among pathogenic mycobacteria but remarkably absent from non-pathogenic species which could be an initial indication that it plays an essential role in *M. tuberculosis* survival (Cha & Cooksey, 1991). It contains a N-terminal signal sequence typical of prokaryotes within the first 38 amino acids (Rowland & Nieoderweis, 2013). Previous studies indicated that the *M. tuberculosis'* MmcO signal peptide can lead to localization of MmcO to the pseudo periplasmic space, similar to many other bacterial multi-copper oxidases such as *Pseudomonas syringae* CopA, and *C. jejuni* MmcOC. MmcO has a wide range of organic substrates like Fe (II) and phenolic compounds (Rowland & Nieoderweis, 2013). MmcO oxidation results in a single-electron that combines with oxygen to be reduced to water. This demonstrates that MmcO activities need oxygen. MmcO has a total of four copper ions which are coordinated in central sites: these are Type 1 copper (Cu1); Type 2 (Cu2) and a pair of type 3 (Cu3) copper. Since MmcO substrate oxidation takes place at Cu1, Cu1 is the mononuclear center that coordinates with cysteine to make MmcO blue in color. The electrons resulting from this oxidation reaction are transferred to the trinuclear center comprising Cu2 and the pair of Cu3 where the reduction of oxygen to water takes place (Figure 5) (Quintanar et al., 2007). *M. tuberculosis'* MmcO has proven to be a virulence factor against host copper toxicity; nonetheless, studies on the role of MmcO in the respiratory burst are limited or non-existent, which is what this study is focused on.

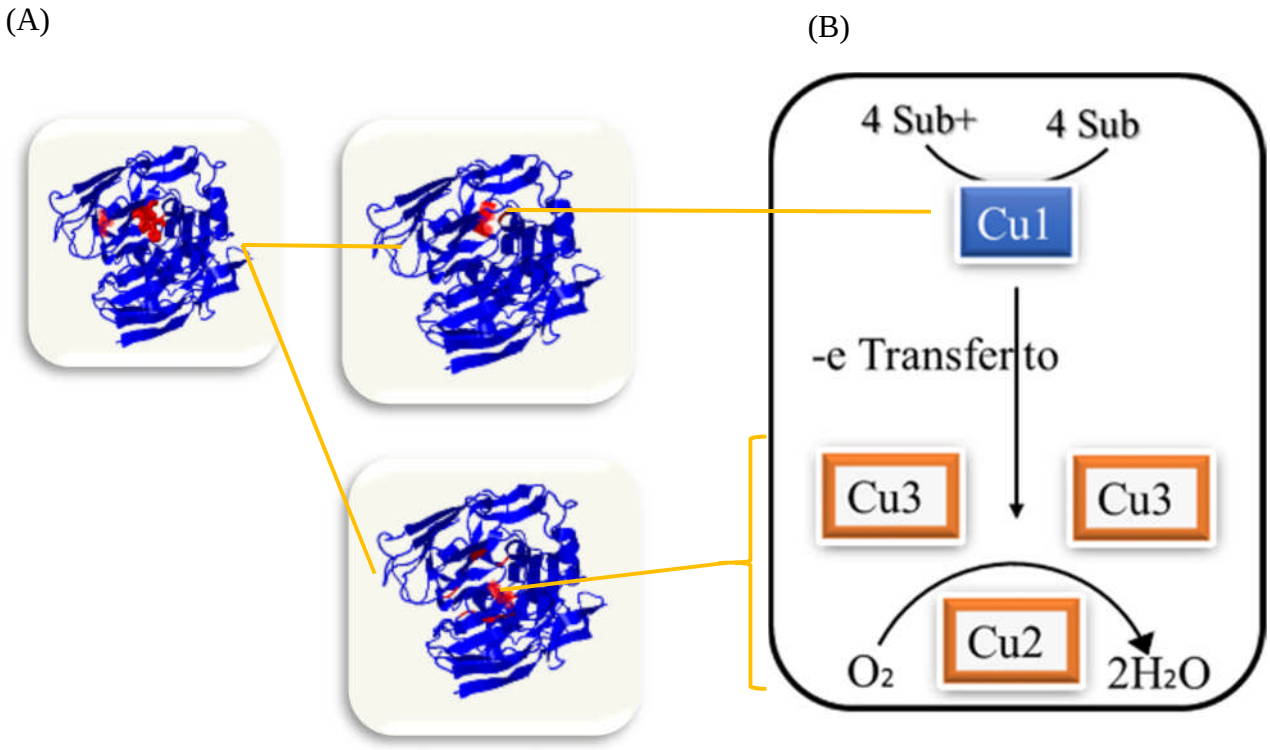

Figure 5: Multi copper oxidase structure: (A) The three dimensional structure of MmcO (adapted from Phyre2 program) and the Figure also shows the active site with the determination of the oxidation center (Cu1) and reduction center (Cu2 and pair of Cu3). (B) Schematic of the MmcO' catalytic mechanism; which the single-electron oxidation of a substrate and the subsequence reduction of oxygen molecule into water.

Rationale

M. tuberculosis is a pathogenic bacterium causing severe TB disease that kills approximately 1.5 people annually. New aspects to the pathogenicity of *M. tuberculosis* continue to be discovered. Studies indicated that *M. tuberculosis* strains became drug resistant to single drugs but the combination of at least two drugs or more shows greater efficacy. However, *M. tuberculosis* has evolved to develop multidrug resistance strains over time. It is known that *M. tuberculosis* cell wall components and the secretion enzyme system are crucial defensive mechanisms against the host innate immune system including macrophages in which antimicrobial activity is defined by the respiratory burst. In this case, understanding the role of different virulence factors in its pathogenicity could lead to better therapeutic strategies. *M. tuberculosis* Multi Copper Oxidase (MmcO) is considered as a virulence factor. A recent study has indicated MmcO as a virulence factor in resistance to copper toxicity but the role of MmcO in response to macrophage respiratory burst requires more work (Rowland & Nieoderweis, 2013). MmcO contains copper, and copper type 2 (Cu2) has proven its ability to neutralize and reduce superoxide ($O_2^{\bullet -}$) into oxygen (Gaetke & Chow, 2003). This makes the MmcO a good candidate to suppress/ prevent the release of ROS. In addition, MmcO possesses the capability of consuming and reducing oxygen molecules to water (Heppner et al, 2014). O_2 molecules are required in ROS-production as well as MmcO activity, leading to the possibility of MmcO competing with NADPH oxidase for O_2. Therefore, we will investigate if MmcO plays a role in the inhibition of the phagocytic respiratory burst in THP-1 cell line. THP-1 is defined as a human monocytic cell line module, which was obtained from a one year old male patient suffering from acute monocytic leukemia (Adati et al, 2009). We hypothesised that MmcO has the capability of interfering with ROS formation during the phagocytic respiratory burst and this contributes to the survival of *M. tuberculosis.*

Objectives

The main research objective of this study is to characterize the *M. tuberculosis* multi-copper oxidase's potential role in interfering with the formation of ROS by using the THP-I monocyte cell line with biochemical assays and proteomics methods. The specific objectives are:

1. The cloning of *M. tuberculosis rv0846c* gene in pET21-a vector
2. The expression of protein in *E.coli* BL21.
3. The purification of recombinant MmcO.
4. The study of MmcO involvement in interfering with the production of ROS in the THP-1 cells.

MATERIAL & METHODS

Cloning of the M. tuberculosis multi-copper oxidase

The sequence of the multi-copper oxidase (*rv0846c*) gene from H37Rv strain was obtained from Tuberculist 2.6 database [http://tuberculist.epfl.ch/quicksearch.php?gene+name=Rvo846c] and National Center for Biotechnology Information (NCBI) website [http://www.ncbi.nlm.nih.gov/gene/?term=Rv0846c]. The primers that were used to amplify the Rv0846c gene were designed by Primer-BLAST [http://www.ncbi.nlm.nih.gov/tools/primer-blast/]. The Forward primer (FP) is [$^{5'}$ **AATAAT***GATCTC*ATGCCCGAGCTGGCCACG $^{3'}$] and the Revers primer (RP) is [$^{5'}$ **AATAAT***CGCCGGCG**CGGCGGCGGCGG*CCCCAGAATGTAGTCCAG $^{3'}$]. Both of these primers contain restriction sites (red), overhang nucleotides (bolded black), and a linker (green). The primers were synthesised by Invitrogen Life Technologies. The *rv0846c* gene was designed as a fusion construct with a 6xHis tag at the C-terminus by a glycine linker (Figure 6A). A linker consisting of 9 glycines, 4 were created by the reverse primer and 5 were part of the pET21a vector, was used. The amplification of *rv0846c* was carried out using a polymerase chain reaction (PCR), Q5 High fidelity polymerase kit, and the pair of primers. The composition of each 25 µl of reaction was as follow: 1X Taq buffer, 25 mM $MgCl_2$, 100 µM dNTP, 20 nM forward and reverse primers, 2.5% DMSO, 50 ng DNA and 1unit Q5 High fidelity Taq polymerase [New England Biolabs (NEB)]. *M. tuberculosis* H37Rv strain genomic DNA, which was used as template in this study, was synthesised by GenScript Company. The PCR reaction begins with a denaturing step for 5 min at 95°C, followed by 35 cycles at 94°C (for1 min) and at 62°C (for 40 s) [which is the optimal annealing temperature based on NEB calculator and our optimization], and an extension period for 1.30 min at 62°C followed by a 10 min extension at 72°C. The PCR products were examined by

electrophoresis as a conformational step. A sample of 5 µl from each reaction was subjected to electrophoresis on 1% agarose gels containing 0.5 µg/ml ethidium bromide. Samples were loaded with 6X loading dye [Fermentas] and they were run in 1X TAE running buffer [Promega] for one hour at a constant voltage of 100 V. The gels were visualized using a UV trans illuminator [chemidoc xrs Bio-RAD]. The PCR product was then cloned into a bacterial expression plasmid known as pET21a [GenScript] (Figure 6B). Both PCR product and pET21a plasmid were subjected to double digestion by two different restriction enzymes (NdeI and NotI) [NEB]. Both were treated separately with 1µl of each restriction endonuclease (NotI (10 U/µl) and NdeI (10 U/µl)) that mixed with 2µl of 10x Digestion buffer [Fermentas] in a total reaction volume of 20 µl. The mixture was incubated at 37°C for 2 h followed by heat inactivation at 80°C for 10 min. The *MmcO* and the pET21a vector were mixed with T4 DNA ligase [NEB] in a total volume of 15 µl at a ratio of 1:3 (plasmid to insert respectively) after they were cleaned up using EZ-10 spin DNA clean up columns [Bio Basic Inc]. The ligation reaction was kept at room temperature (RT) for 30 min then placed at 4°C overnight.

Transformation of *Escherichia coli* BL21

BL21 strain of *E. coli* was cultured in Luria Bertani (LB) [Fisher Scientific] antibiotic-free media and incubated in a rotary shaking incubation [Forma Scientific] at 37°C/250 rpm for 12 h. The bacterial pellets were resuspended in 0.1 M $CaCl_2$ [Sigma] and then the mixture was incubated for 1 h. At the end of the incubation period, the cells were centrifuged and the pellet resuspended

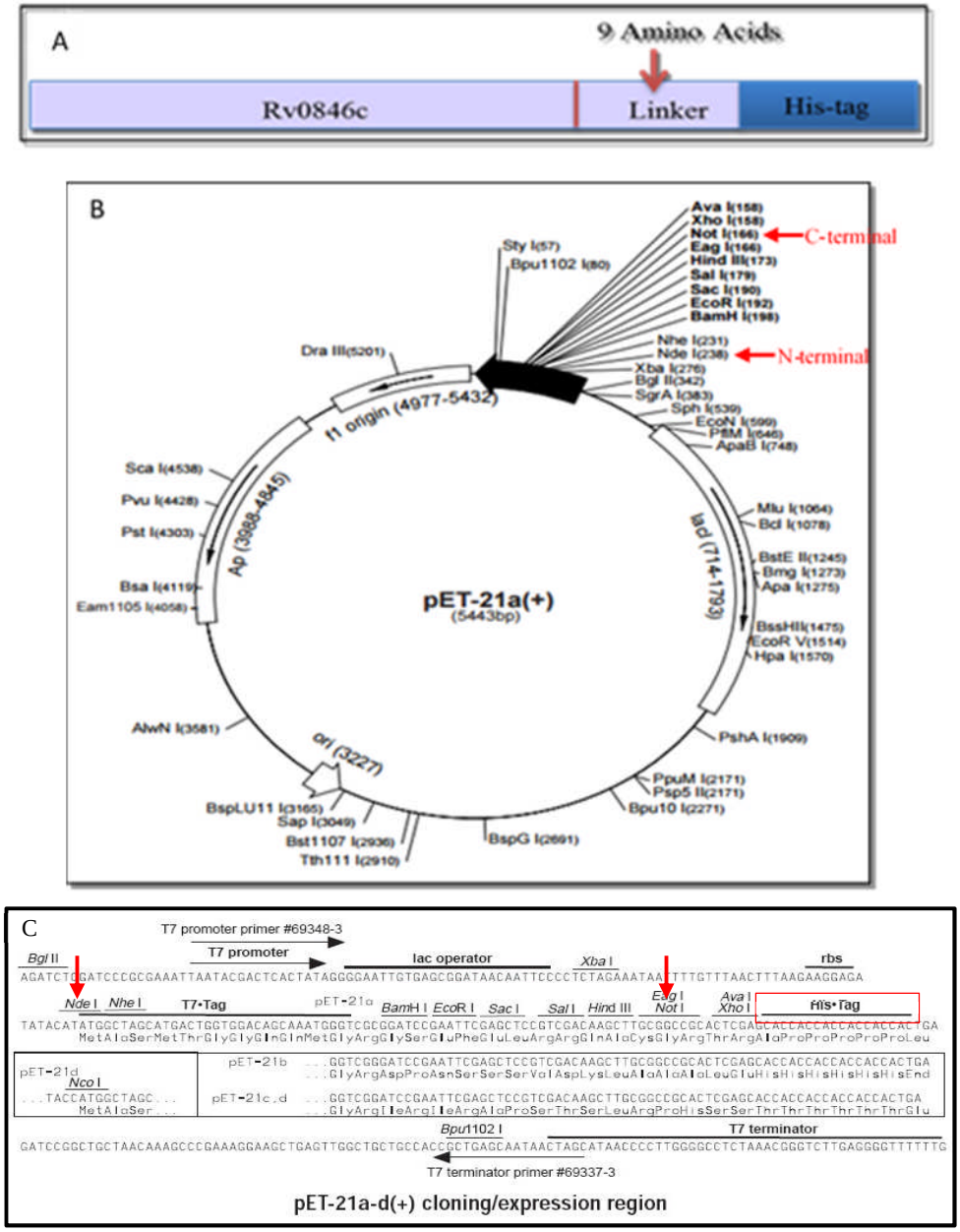

Figure 6: pET21-a plasmid construct: (A) shows the Rv0846c gene design containing N-terminal Rv0846c gene followed by Linker and C-terminal His-tag. (B) represents the pET21a vector construct and the cloning site between (NdeI and NotI) restriction sites. (C) indicates the His-tag location on the plasmid. This Figure is adapted from https://www.addgene.org/20377/.

in 0.1 M cold $CaCl_2$ to the final volume of 1 ml. The cells, perceived to be competent, were placed on ice ready for transformation. The BL21 strain of *E.coli* is commonly used as an expression host for proteins. The transformation was performed following NEB manufacturer's instructions with some modification. 200 µl of BL21 competent cells were mixed with 2 µl ≃ (10 ng) of the ligation reaction mixture in a 1.5 ml micro-centrifuge tube. The sample was flicked gently and incubated on ice for 30 min. The bacteria were then heat-shocked at 42°C for 90 s under different conditions as follows: in a water bath for 40 s, and then immediately in a hot plate for about 50 s. Finally, the sample was placed on ice for a further 5 min. For recuperation, 800 µl of sterile, antibiotic-free SOC media (2% tryptone (w/v), 0.5% yeast extract (w/v), 10 mM NaCl, 2.5 mM KCl, 10 mM $MgCl_2$, and 20 mM glucose) [all components were from Fisher Scientific] was added and the sample was incubated on an incubator-shaker [Forma Scientific] for 45 min at 37°C and 250 rpm. Individual colonies were isolated by plating 100 µl of the sample on a selective LB agar plate (2.5% LB broth, 1.5% agar [Fisher Scientific]) supplemented with 100 µg/ml ampicillin [ThermoFisher Sci.] and incubated for 12 hours at 37°C.

Protein expression, inclusion bodies extraction and MmcO refolding

The transformed bacteria was cultured in 5 ml LB media supplemented with 100 µg/ml ampicillin at 37°C/250 rpm for 12 h. 600 µl of this culture was added to 1 L LB media and grown at 37°C in a rotary shaking incubator at 250 rpm until the optical density (OD_{600}) of the culture was 0.5-0.8 (about 2 h). Then 0.4 mM isopropyl β-D-1-thiogalactopyranoside (IPTG) [Sigma] was added and the culture was grown for a further 6 h at 35°C/250 rpm. At the end of the 6 h, the culture was ready for protein extraction. The extraction of the recombinant protein from inclusion bodies was performed in a similar way to experiments conducted by Rudolph and Lilie in (1996).

In brief, the culture was centrifuged to obtain a cell pellet at 4°C/14,000 xg [Avanti J-52I centrifuge, Beckman Coulter] for 20 min. The cell pellet was resuspended in 20 ml Lysis buffer containing 50 mM Tris-HCl pH 8.00 [Fisher Scientific], 25 mM NaCl [Fisher Scientific], 5 mM EDTA [Bio Basic], and 1% Triton X-100 [Sigma] (v/v), per gram wet weight of cell pellet. The suspension was incubated on ice for 30 min and then sonicated for 10 s for 5 cycles at 16 V using a Heat Systems-UltraSonic.inc, W208 Sonicator with 30 s rest on ice in between. The reason for the ice resting time is to protect the extracted proteins from thermal degradation. Sonication prevented clumping of the cells before centrifugation at 4800 xg [Eppendorf Centrifuge 5804 R, Brinkman Instruments. Inc] and 4°C for 35 min. Next, the sample was washed to eliminate all the indigenise protein of the host cell. The washing step was performed three times using 20 ml of buffer A, B, and C. The first wash was done in buffer A (50mM Tris, pH7.5, 50mM NaCl, 50mM EDTA, and 1%Triton). The second wash was performed in buffer B (50mM Tris, pH7.5, 1M NaCl, 50mM EDTA, and 1%Triton). The last wash was done in buffer C (50mM Tris, pH7.5, 50mM NaCl, 50mM EDTA). The pellets were then resuspended in 10 ml solubilisation buffer which included 8 M Urea [Fisher Scientific], 1 mM phenylmethane sulfonyl fluoride (PMSF) (v/v), 50 mM Tris-HCl pH 7.5, and 5 mM dithiothreitol (DTT) [Sigma] and incubated to disrupt the pellets inclusion by additional shaking of the solution for 12 hours at RT.

To promote protein refolding, the solubilised sample was centrifuged at 4°C and 4800 xg for 35 minutes, and then the 10 ml supernatant was transferred to dialysis tube, and subjected to dialysis in 500 ml 10 mM Tris-HCl pH 7.4. This technique was used to gradually remove the denaturant Urea so as to refold the denatured proteins. The dialysis was performed at the RT by placing the dialysed beaker on the stirrer plate and changing the 500 ml dialysis buffer 3 times with an interval of two hours. The last change of dialysing buffer was 1 L for a period of 12 h.

Finally, the dialysate was subjected to centrifuge at 4°C and 12,000 xg for 5 min to isolate the refolded protein in the pellet.

Protein purification using nickel affinity chromatography

The purification of the recombinant His-tagged MmcO protein was carried out using a 1 ml Nickel column (Ni) [GE Healthcare Life Science] according to the GE Healthcare Life Science manufacturer's instructions. In brief, the purification was carried out in two steps. First, the refolded protein was first desalted on 26/10 desalting column [GE Healthcare Life Science] and eluted with 20 mM $NaSO_4$, 0.5 M NaCl, and 25 mM Imidazole v/v, which is the Nickel column' binding buffer. Second, the 1 ml Nickel column was conditioned with 20 ml of the binding buffer and then the desalted sample was applied at a flow rate of 1 ml /min (saved as the flow through fraction) and the column washed with 20 column volume of binding buffer. The bound protein was eluted in 10 column volume of elution buffer (20 mM NaP "nickel resin", 0.5 M $NaCl_2$, and 500 mM Imidazole) and concentrated using an Amicon spin unit/Nitrogen with 10 kDa cut off cellulose membrane and equilibrated with 10 mMTris-HCl (pH 7.4). The protein concentration was measured using the Bradford Protein Assay Kit [Bio-Basic] with bovine serum albumin as the standard (according to manufacturer instructions). This is a colorimetric assay that measures the protein concentration based on the Coomassie Brilliant Blue dye-binding method. Protein solution was prepared in duplicate and the intensity detected at 595 nm on a MRX Microplate Reader. Protein concentrations were determined from the standard curve.

Sodium dodecyl sulfate polyacrylamide gel electrophoresis (SDS-PAGE)

Denaturing SDS-PAGE gels were prepared as described by Hames (1998). In brief, SDS-PAGE gels consisted of a 10% separating gel (2.5 ml 40% polyacrylamide, 2.5 ml 1.5 M Tris-HCl, pH 8.8, 100 µl 10% ammonium persulfate, 100 µl 10% SDS, and 4 µl tetramethylethylenediamine (TEMED) (v/v)) and a 5% stacking gel (500 µl 40% polyacrylamide, 500 µl 1 M Tris-HCl pH 6.8, 40 µl 10% ammonium persulfate, 40 µl 10% SDS, and 4 µl TEMED (v/v)). Once the gel completely polymerized, the protein samples (5-40 µg) were combined with 4X Laemmli sample buffer (44.4% glycerol, 4.4% SDS 0.1 M Tris-HCl pH 6.8, 0.02% bromophenol blue w/v, and 10% β-mercaptoethanol v/v), boiled at 95°C for 5 minutes, and then loaded into the wells. The gels subjected to electrophoresis for 45 min at a constant voltage of 100 V using a Mini-PROTEAN Tetra System [BIO-RAD] with 1X SDS running buffer (144 g glycine [Sigma], 1/10 dilution of 30 g Tris-HCl, pH 8.3,10 g SDS in 1 L). The gel was stained with Coomassie brilliant blue R-250 (methanol, acetic acid) stain for visually documentation.

Western blot

The western blot was performed as described by Mahmood & Yang (2012) with some modifications. In brief, the proteins were transferred to a 0.22 µm PVDF membrane [GE Healthcare Life Science] rinsed in 100% methanol. The PVDF membrane and 10% SDS-PAGE were sandwiched between two thick blot pads previously soaked in 1X transfer buffer (30.2 g/L Tris-HCl, pH 8.3 and 144 g/L glycine [Sigma]) and the protein transferred using a semi-dry apparatus [Bio-Rad Trans-blot] at constant voltage (15 V) for 35 min. After transferring, the membrane was blocked by incubation in blocking solution (5% skim milk in 1X PBST buffer

contains 8 g/L NaCl, 0.2 g/L KCl, 1.44 g/L Na_2HPO_4, 0.24 g/L KH_2PO_4 and 0.05% Tween-20) at 4°C with shaking for 12 h. This membrane was rinsed 3 times in 1 X PBST and then probed by incubation with the primary anti-His-tag antibody [Gen Script] at a 1/3000 dilution in 5% milk in 1 X PBST at RT with shaking for 2 h. The membrane was washed 3 times in 1 X PBST and then probed with the secondary, anti-rabbit IgG alkaline phosphatase conjugated antibody [Biomeda] at 1/30000 dilution at RT with shaking for 2 h. For the last time, the blot was washed three times for 5 min with 1 X PBST and once with 1X PBS followed by the detection of the bond attached using 0.8 mg 5-bromo-4-chloro-3-indolyl phosphate (BCIP) and 1.2 mg nitro blue tetrazolium (NBT) in 10 ml of detection buffer (1MTris-HCl pH 9.6, 1M $MgCl_2$). After the desired band appeared, the membrane was left to dry and the visually appearance of the targeted band documented.

MmcO activity measurements

The MmcO activity assay is based on oxidizing the ABTS (2,2'-azino-bis-3-ethylbenzthiazoline-6-sulphonic acid) substrate [Sigma-Aldrich] to the ABTS• radical to generate a green-blue color by the action of MmcO protein. This assay was performed as described previously with modification (Grass & Rensing, 2001). In brief, the assay was carried out using a Costar 96-well flat bottom plates and a volume of 200 µl. 20 µg (equivalent to 0.327 nmol) of MmcO protein was added to 50 mM Sodium acetate [Sigma] buffer, pH 4 containing 2 mM ABTS and 2 mM $CuSO_4$ [Sigma]. The plate was sealed and incubated at RT with shaking for 4 h. The activity readings were taken every 30 min for 4 h. Finally, the absorbance of the ABTS formed was measured at 405 nm using a MRX Microplate Reader. Specific activity was calculated using $A = \varepsilon lc$ where A= absorbance, ε = 18,400 M^{-1} cm^{-1} ,1 = 0.58cm, and c= concentration of the

solution. One unit of enzyme activity is defined as the amount of enzyme required to oxidize 1 µmol ABTS in 1 min.

Delivering MmcO into THP-1 cells

The THP-1cell line was generously provided by Dr. Robert Lafrenie (Health Science North Research Institution, Sudbury, Canada). THP-1 is characterized as a large rounded single nonadherent cell. It is a phagocytic cell that can be differentiated into macrophage cells using phorbol 12-myristate 13-acetate (PMA) (Tsuchiya et al, 1980). THP-1 cells were cultured as described by Walev et al, (2001) with some modification. In brief, culturing of the cells were conducted in Corning® T-75 flasks in GI-1640 Medium [Hyclone] with 10% Fetal Calf Serum (FCS) [Hyclone], and 1X 100 µg/ml streptomycin and 100 unit/ml penicillin [Life Technologies] at 37°C and 5% CO_2. The cells were cultured by the addition of a fresh media every 2 or 3 days. The viability of the cell was constantly checked by microscopy check using Trypan Blue stain [Bio rad] and to ensure the concentration of the cell remains below $1x10^6$ cell/ml. Pores were formed in the plasma membrane of the THP-1 cells using 20 ng/ml Streptolysin-O (SLO) [Sigma] and 200 µl of ~$9x10^6$ THP-1 cell/sample in the presence of 50 µg/ml Fluorescein Isothiocyanate Conjugated (FITC)-albumin [Sigma]. This procedure was performed in several steps. The first step involved the activation of SLO through the incubation of a 1 µl SLO from 1 mg/ml stock in activation buffer (20 mM/l 4-(2-hydroxyethyl)-1-piperazineethanesulfonic acid (HEPES), 20 mM/L DTT, and 1X PBS up to 1 ml) at 37°C for 10 min. The second step involved the preparation of the cell suspension. In this step, 160 ml of $1x10^6$ per ml THP-1 cell culture were centrifuged at 22°C and 400 xg for 10 min and the resulting pellets washed two times with serum free GI media followed by resuspension of the pellets in about 3 ml of serum free GI media. In the final step, the

cell suspension and the activated SLO were mixed in the presence of different concentrations of MmcO. The cells ($9x10^6$ cells/200 µl) were divided into 2 sets of 7 tubes: five of the tubes contained 1 µl of 20 ng/ml SLO, 1 µl 50 µg/ml FITC-albumin, and MmcO concentrations of 0,10 ng, 100 ng, 250 ng, and 500 ng; one tube contained 1 µl 50 µg/ml FITC-albumin and 500 ng MmcO (without SLO); and one tube contained 1 µl 50 µg/ml FITC-albumin only. Then the samples were incubated at 37°C for 15 min. After the formation and the permeabilization in the presence of MmcO, the pores were sealed by treating the cell pellets with ice cold RPMI media supplemented with 10% FCS, 1 X of 100 µg/ml streptomycin and 100 unit/ml penicillin in addition to 2 mM $CaCl_2$. The samples were then incubated at 37°C for a further 1 h. As a confirmation of the occurrence of the permeabilization and resealing of the cells, 5 µl of each sample were examined using confocal microscopy to demonstrate the FITC-BSA was present in the cell cytoplasm. Finally, the samples for each set were pelleted and suspended in 200 µl of serum free RPMI media.

Measurement of Reactive Oxygen Species (ROS)

The ROS assay was carried out using ROS-Glo™ H2O2 Assay kit [Promega]. This assay is based on measuring the amount of hydrogen peroxide (H_2O_2) produced after treatment with a ROS inducer using a H_2O_2 substrate. The reaction between H_2O_2 and its substrate result in the production of Luciferin which generated a light signal in the presence of recombinant luciferase (Figure 7). A microfluor®1 96-well white plates was used in the performance of the ROS assay which was done in duplicate in a volume of 100 µl. This assay was performed as described in the manufacturer's instructions supplied with the kit. In brief, 80 µl each of the individual 14 samples was transferred each well of a 96-well white plates containing 20 µl H_2O_2 substrate. A separate

set of wells also contained 1 µl 50 ng/ml phorbol 12-myristate 13-acetate (PMA) as the ROS inducer. The plate was then incubated at 37°C for 30 min followed by treatment with a detection buffer at RT for 20 min. The measurement of the ROS production was carried out using a Synergy H4 Hybrid Reader Luminescence reader for 5 s per well.

Statistical analysis

The statistical analysis for the measurement of ROS production (permeabilized/non permeabilized and induced/uninduced cells) was carried out using one-way ANOVA software [http://turner.faculty.swau.edu/mathematics/math241/materials/anova/]. The raw data of ROS concentration for three independent experiments performed in duplicate were uploaded on one-way ANOVA. Tukey's software [http://faculty.vassar.edu/lowry/hsd.html] was then used to determine the actual differences between the MmcO concentrations. All data uploaded are the mean ± standard error.

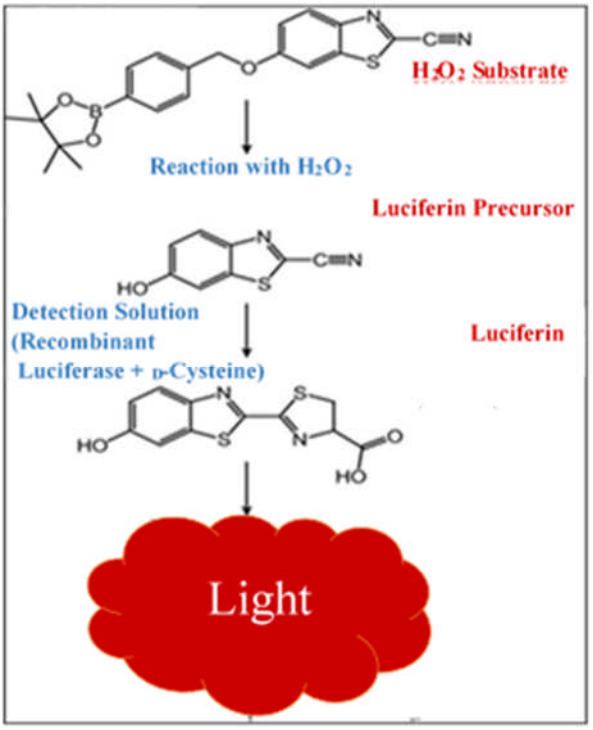

Figure 7: Principle of the ROS sssay: H_2O_2 converts the supplied H_2O_2 substrate to a luciferin precursor, which is then converted to luciferin before the addition of a second reagent containing recombinant luciferase and D-Cysteine. Finally, the presence of recombinant luciferase converts the luciferin into a luminescent product. This Figure is adapted from ROS-Glo™ H_2O_2 Assay kit (Promega Corp.).

Results

Cloning and expression of MmcO

Based on the obtained information from Tuberculist 2.6 and NCBI databases, the *M. tuberculosis* Rv0846c gene is identified as a probable oxidase or oxidoreductase protein and recently it has been confirmed as a membrane associated multi-copper oxidase (MmcO) according to Rowland and Niederweis (2013). MmcO contains 504 amino acids (1515 bp) and a molecular weight of approximately 54 kDa in its mature form (signal peptide cleaved). For the purpose of this study, the expressed MmcO had a 9 amino acids linker and a 6x His tag added at the C-terminus which increased the molecular weight to ~61 kDa (signal peptide unprocessed in *E. coli* during expression).

MmcO is functionally characterized for its oxidoreductase activity and the catalytic site has been located to cysteine 486 which is essential for MmcO activity (Rowland and Niederweis, 2013). MmcO contains two cysteines, the second at position 35 anchors the protein to the membrane via lipidation (McDonough et al., 2008). The signal sequence at the N-terminus of the protein is in fact a Tat signal sequence, implying processing through the Tat translocon in the cytoplasmic membrane instead of the Sec translocon (McDonough et al., 2008). The signal sequence is 34 amino acids long ending with LAA cleavage site (Figure 8). The cysteine immediately following the cleavage site is the cysteine most likely modified with lipidation to anchor the protein to the membrane.

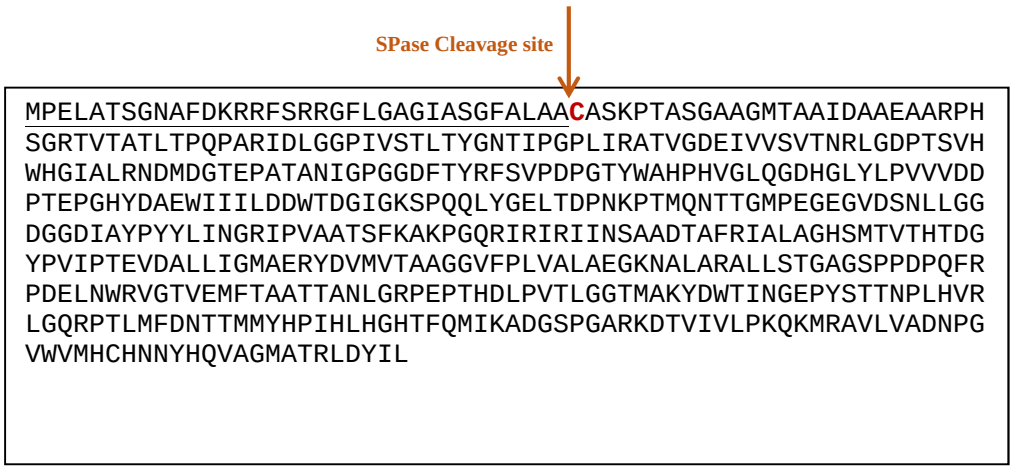

Figure 8: MmcO amino acid sequence: underlined is the Tat signal sequence ending with the LAA cleavage site at amino acid 34 (arrow). The cysteine proposed to be the site of lipidation is highlighted in red at position 35.

The *rv0846c* gene was amplified from *M. tuberculosis* H37Rv genomic DNA using PCR. The successful amplification involved the use of an optimal annealing temperature of 62°C. A single band with an appropriate size of 1557 bp, which corresponds to the predicted size of *rv0846c* gene, was resolved on a 1% agarose gels supporting the efficient amplification of *rv0846c* (Figure 9). The PCR product could be demonstrated as fragments by cutting the recombinant plasmid with NdeI and NotI which appeared as double bands, a band at ~1600 bp (the insert) and the another one around the ~5500bp (host plasmid) which were visualized on 1% agarose gels (Figure 10). These fragments determined the successful cloning.

Protein Extraction and Purification

Localization of the expressed MmcO

Determination of the cellular localization of expressed MmcO is the most important step. Different extracts from different subcellular compartments including cytoplasmic, periplasmic, and inclusion bodies were isolated and separated on 10% SDS-PAGE gel and subjected to western blot analysis versus a negative control (the untransfected host cell BL21). The Figure 11A shows that the MmcO expected band was found to be at ~61 kDa; however, this band was only present in the pellet of an inclusion bodies extracted with 4% SDS. The western blot showed anti His-tag, (anti His-tag combined to anti-rabbit IgG alkaline phosphates conjugated antibody), reactive band at 61 kDa corresponding to MmcO size (Figure 11B PVDF membrane). Thus, we decided to extract the MmcO protein from the inclusion bodies. However, using SDS to extract the MmcO protein was ineffective because SDS inhibits MmcO activity (More et al, 2011). In addition,

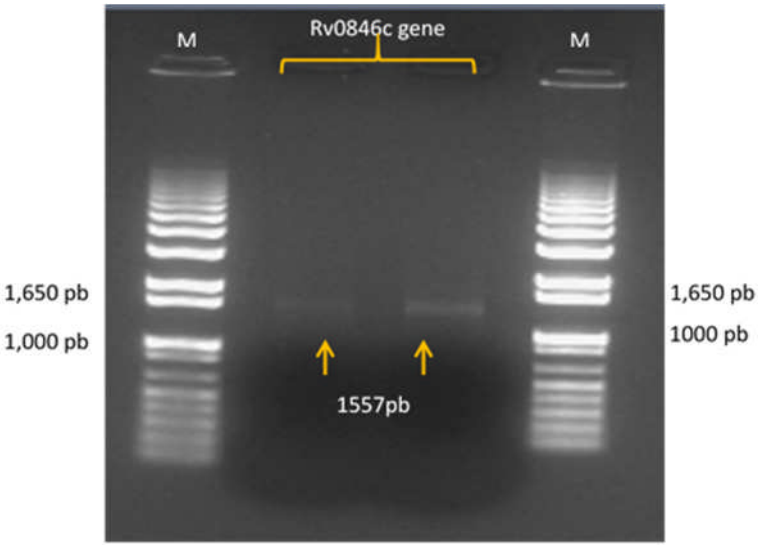

Figure 9: *rv0846c* gene product from the PCR. The arrows on 1% agarose gel indicate the actual size of Rv0846c gene product at 1557 bp after the PCR, M=marker

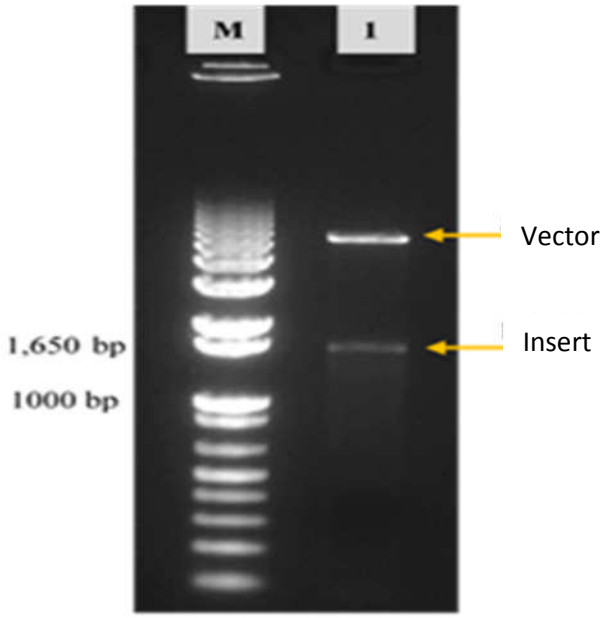

Figure 10: Double digestion after cloning. 1% agarose gel shows in line (1) a double digestion of the construct that results in two bands, insert and empty pET21a plasmid. M=marker.

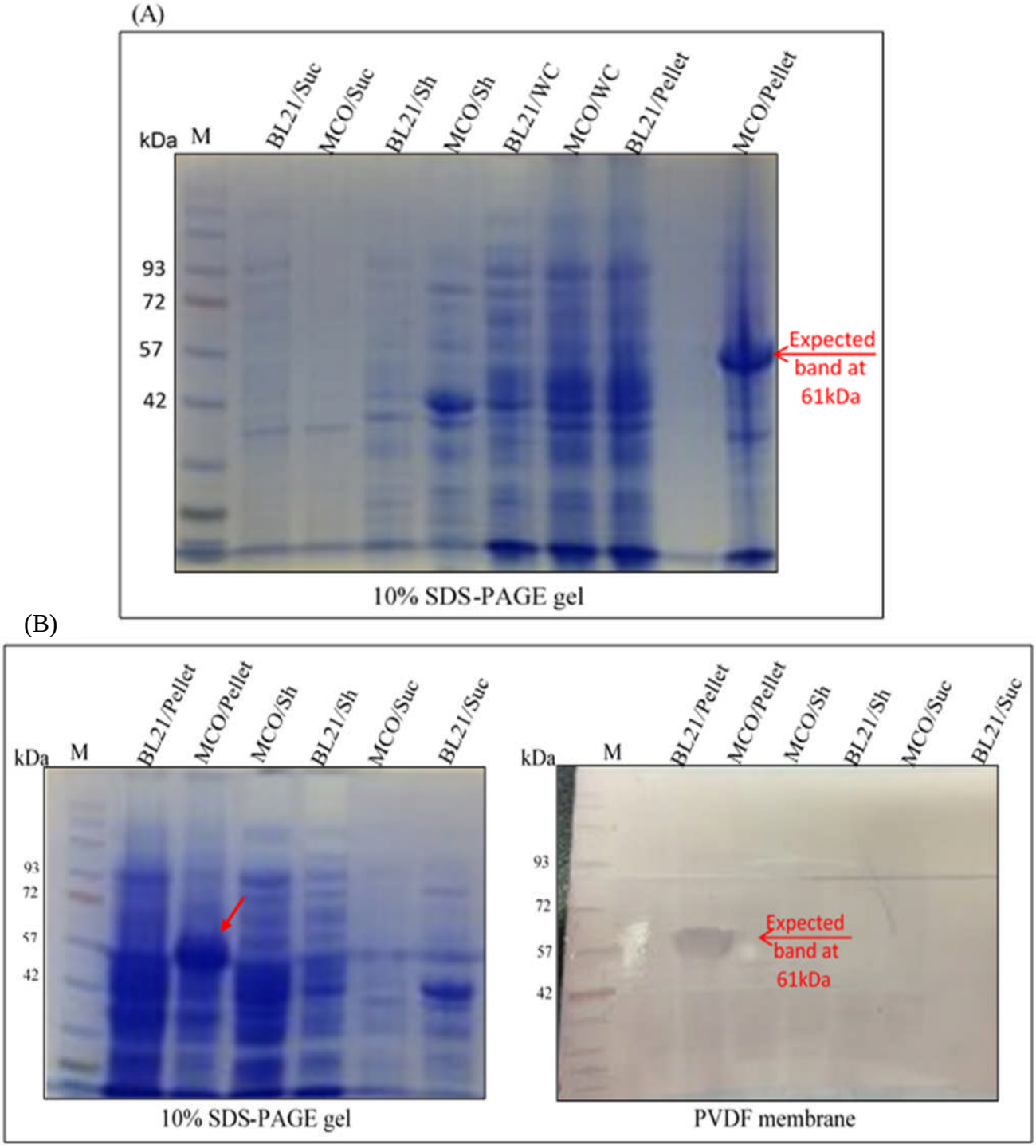

Figure 11: Localization of expressed MmcO in three cell fractions: (A) 10% SDS-PAGE gel stained by Coomassie stain represents the extraction of recombinant MmcO from periplasmic (suc/sh) fraction, cytoplasmic (wc) fraction and inclusion bodies (pellet) fraction. These fractions were compared to the empty *E.coli* BL21 (host).The gel shows that MmcO was expressed and extracted successfully from pellet at the right size of 61 kDa. (B) Both 10% SDS-PAGE gel stained by Coomassie stain and western blot for anti-6xHis tag, show the expected band at 61 kDa and

potential contamination of MmcO's extract with host cell' endogenous proteins could be problematic (Figure 11B SDS-PAGE gel). Therefore, the inclusion bodies extraction protocols were optimized and modified for higher efficiency.

Extraction of MmcO from inclusion bodies

Several attempts to purify soluble and active MmcO from the BL21 expression host have failed. Expression of *MmcO* in the *E. coli* BL21 strain under the T7 promoter resulted in the formation of inclusion bodies, which are an insoluble form of protein, despite the presence of a MmcO signal peptide. In fact, inclusion body extraction methods were used to obtain sufficient and pure protein extracts. To obtain an active MmcO protein, the denaturant urea was used, then gradually removed using dialysis against a buffered solution containing no urea. Based on the previous experiments that were conducted in our laboratory, refolding insoluble proteins in salt buffer reduced the formation of aggregates during the refolding period. As the refolding of MmcO in 10 mM Tris-HCl buffer pH 7.4 was completed, the expected band was visualized via electrophoresis on 10% SDS-PAGE gels and Western blot analysis on PVDF membranes (Figure 12 PC). The gel illustrates double bands (Figure 12 PC); the expected band at the size of 61 kDa and another one at ~130 kDa. However, the PVDF membrane shows only the targeted band (61 kDa) after detection with the anti-His antibody. This result indicates that the single band on the PVDF membrane, which is the actual size of the recombinant MmcO protein, as well as confirms the effective extraction of MmcO protein from the inclusion bodies.

Purification of the MmcO

Although inclusion body extraction resulted in almost purified MmcO protein, absolute purification required addition steps. Therefore, the refolded MmcO sample was subjected to chromatograph on 1ml affinity Nickel column to purify the His-tagged MmcO protein. The affinity purified MmcO protein was detected as a single band at 61 kDa following 10% SDS-PAGE and western blot analysis using anti His-tag antibody (Figure 12, P-MmcO). The flow through fraction was also examined for additional confirmation, which appeared to contain two bands on 10% SDS-Page gel but a single band at 61 kDa by western blot analysis (Figure 12, FT). This indicates the expected band size of MmcO protein but also a contaminating protein. Following affinity purification on nickel-agarose, a single band at about 61 kDa was obtained on gels and western blot membranes. Thus, the above results indicated the successful extraction and purification of MmcO protein.

MmcO activity measurement

The activity of purified MmcO protein was characterised using a widely known oxidation substrate called ABTS. In this experiment, ABTS was oxidised by active MmcO and resulted in a green color. The oxidation of ABTS in 200 µl total reaction volume was measured at 405 nm. The activity of 20 µg MmcO was determined by calculating the MmcO in nmol/min.mg specific activity every 30 min. The greatest activity 47 nmol/min.mg determined after the first 30 min of the incubation period. After one hour, the activity dropped sharply by a half then continued to decrease over 3 h. The last recorded reading indicates less than 10 nmol/min.mg as the graph shown (Figure 13). This result indicates that the MmcO protein is active and that its greatest

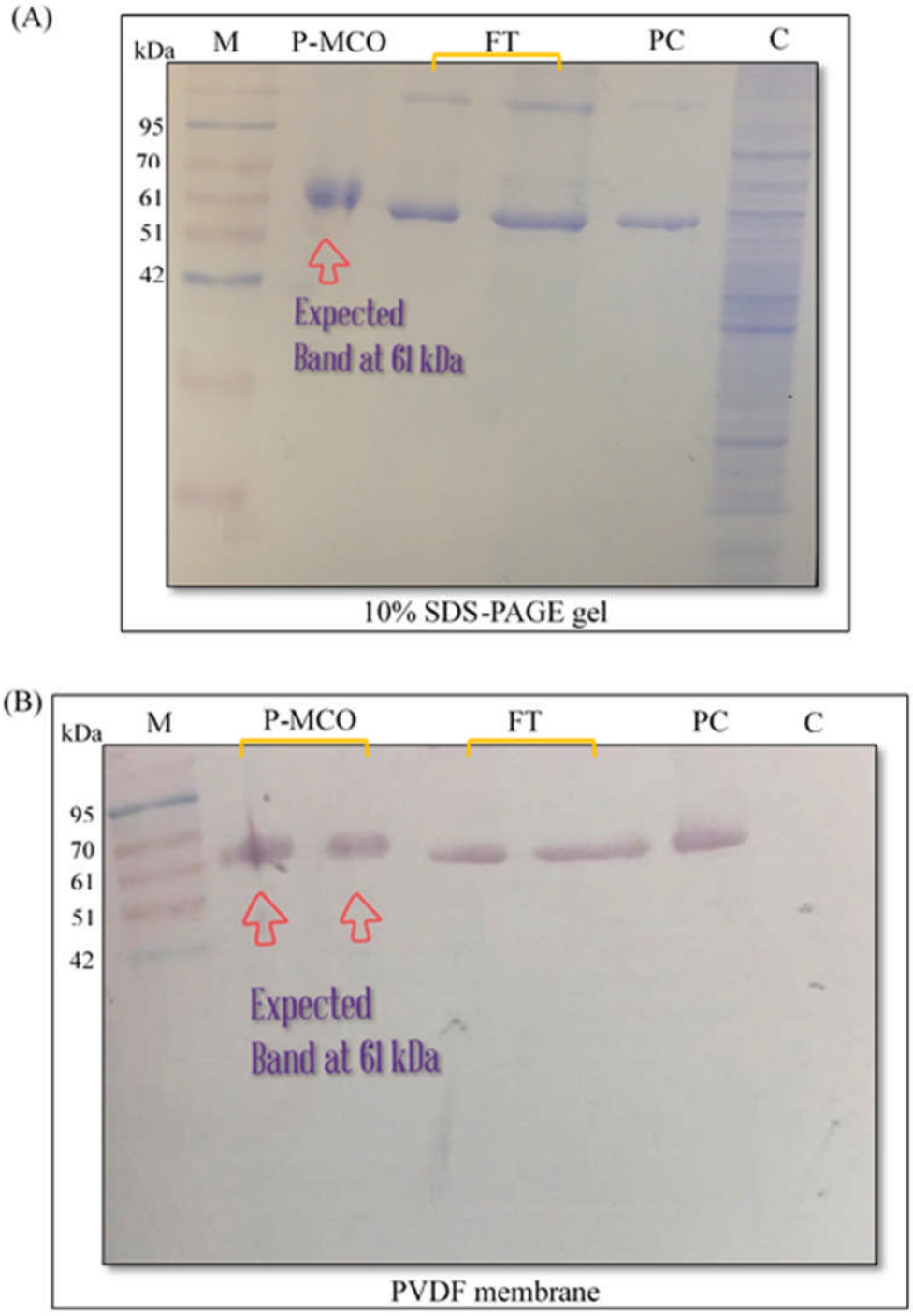

Figure 12: Purification of MmcO extracted from inclusion bodies: (A) 10% SDS-PAGE gel stained by Coomassie stain shows the purified MmcO (P-MmcO) fraction, Flow through (FT) fraction, Pre-column refolded (PC) fraction and those fractions were compared to the empty *E.coli* BL21 cell lysate (lane C). These fractions were run in 40 µg total protein concentration. MmcO was purified successfully and the expected band appears at the right size of 61 kDa. (B) western blot using anti-6xHis tag antibodies. The blot confirms the result from the SDS-PAGE gel. M=Marker

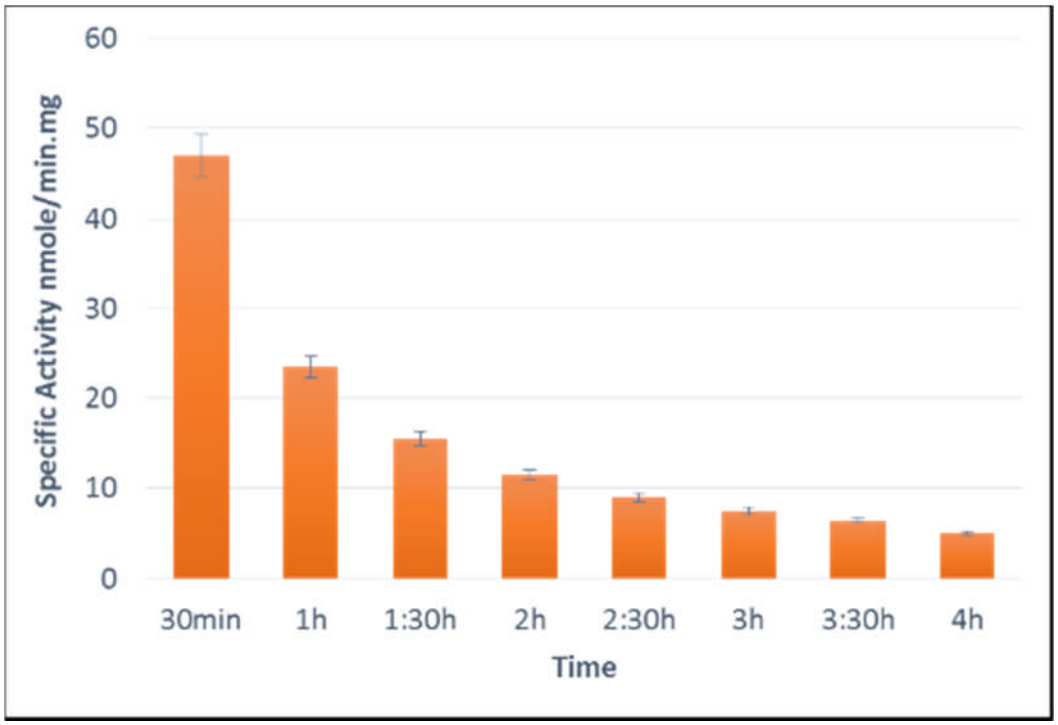

Figure 13: Specific activity of purified MmcO using ABTS substrate: The graph represents the specific activity of purified MmcO over the time using ABTS substrate. The experiment was carried out in triplicates and the values given are the average. Bars represent the mean ± standard error. The high activity of MmcO is detected in the first 30 min of incubation time (47 nmol/min.mg) followed by a gradually decrease for the rest of 3 h.

activity occurs at a period of 30 min of the reaction and also that the MmcO protein loses activity over time.

Delivering MmcO into THP-1 cells

Determination of the effect of the MmcO protein on ROS production was carried out in the THP-1 monocyte cell line. This cell line has been utilized previously by several groups to study ROS production effect in monocyte/macrophages as well as in response to immunological activities (Chanputa et al, 2014). In this study, 200 µl of THP-1 (~$9x10^6$ cell/sample) cells were SLO-permeabilized in the presence of serial concentrations (0 ng, 10 ng, 100 ng, 250 ng, 500 ng) of MmcO protein along with FITC-albumin. Confirmation of successful delivery of MmcO protein in the cells was observed using the FITC-albumin labelling of cells by confocal microscopy (Figure 14). Cells were shown to contain the FITC labelling supporting the idea that proteins in the labelling media were able to enter and become trapped inside the cell using SLO permeabilization method. However, when visualising the fluorescent signals in non-permeabilized cells using confocal microscopy only cell fragments were found to bind label, while the intact cells remained unlabelled (Figure 15). This observation proved that SLO is the permeabilization tool. To confirm a successful MmcO delivery to the cells, the cytoplasmic extract of permeabilized cells was run on 10% SDS-PAGE gel and transferred to a PVDF membrane for western blot analysis. The gel shows THP-1 cells unspecific band from the cell's extract whereas the western blot confirms the presence of MmcO protein (61 kDa) at the 500 ng MmcO lane after the treatment with anti-6xHis tag antibody (Figure 16). Cell viability assessments were routinely carried out using trypan blue exclusion (data not shown).

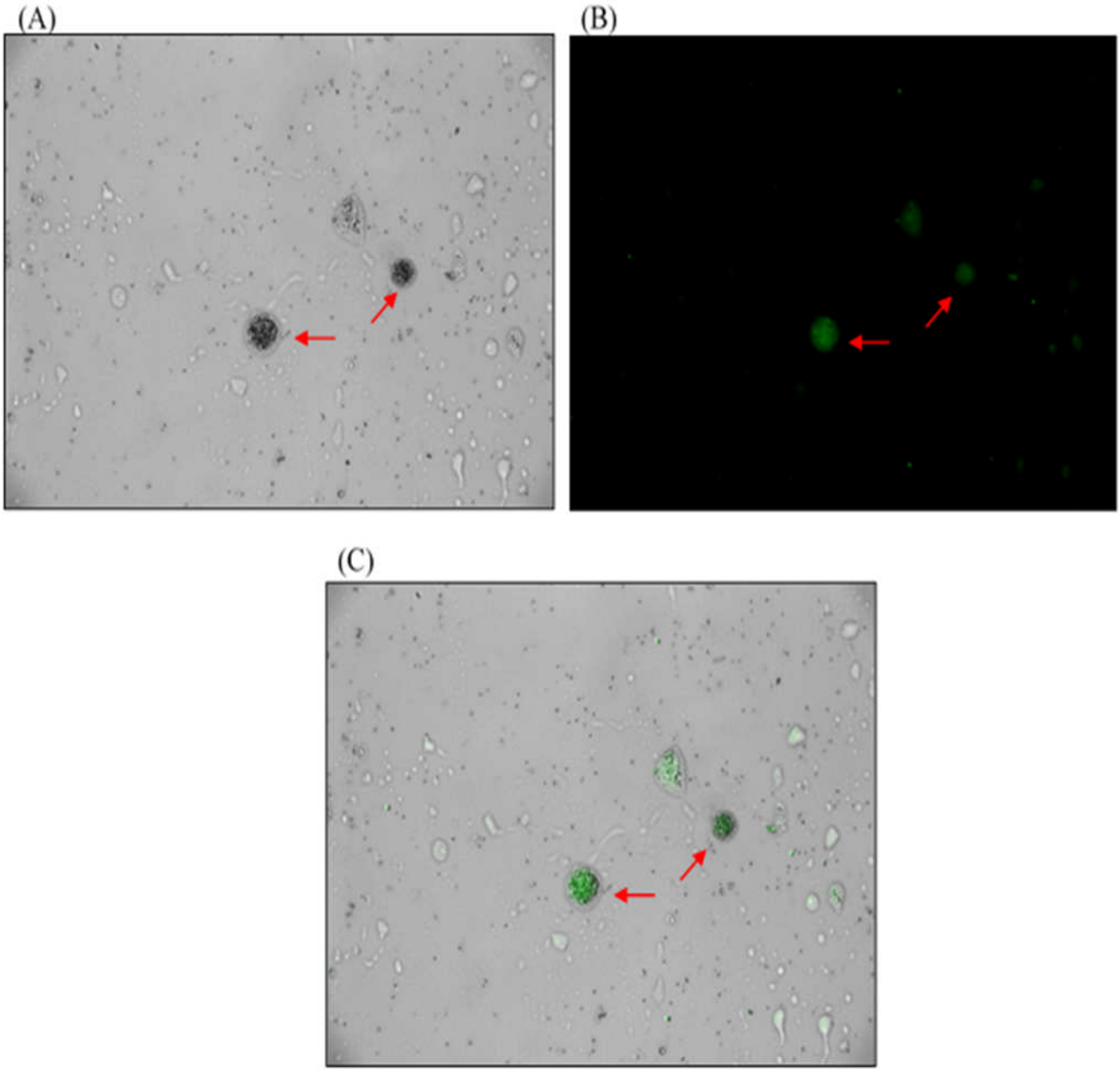

Figure 14: Confocal microscopy images of permeabilized THP-1 cells teated with MmcO: (A) The arrows indicate the THP-1 viable cell shape. (B) Green color represents the permeabilized cells with FITC-Albumin after resealing the membranes. (C) This panel shows the combined images of panels A&B to confirm the green fluorescent light is present inside the cells and not from the background.

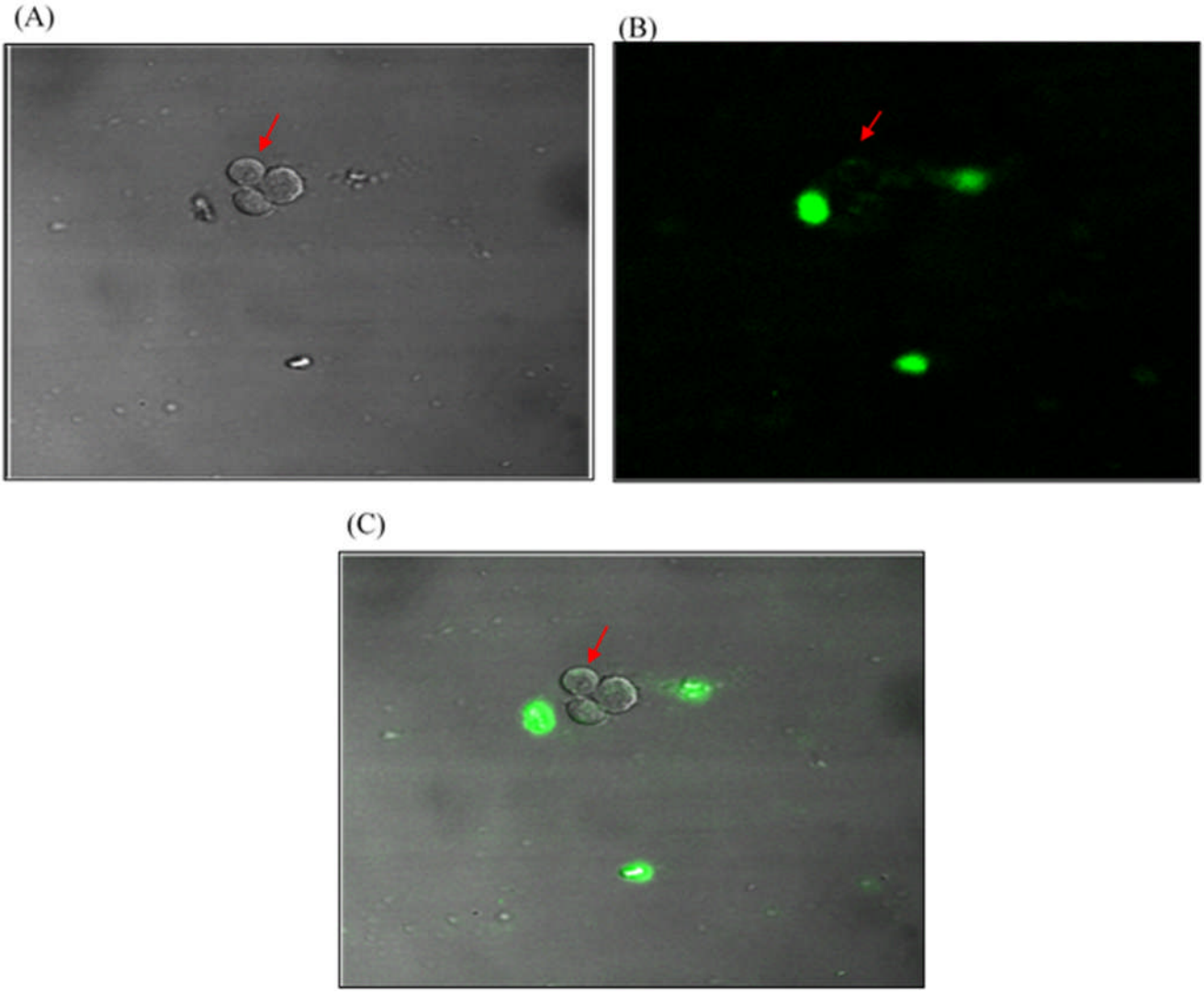

Figure 15: Confocal microscopy images of non-permeabilized THP-1 cells treated with MmcO: (A) The arrows indicate the THP-1 viable cell shape. (B) Fluorescent imaging of the same cells as in panel A. The cells do not display any fluorescence. (C) Combined image of panels A&B to confirm that the green fluorescence in panel B does not originate from the cells.

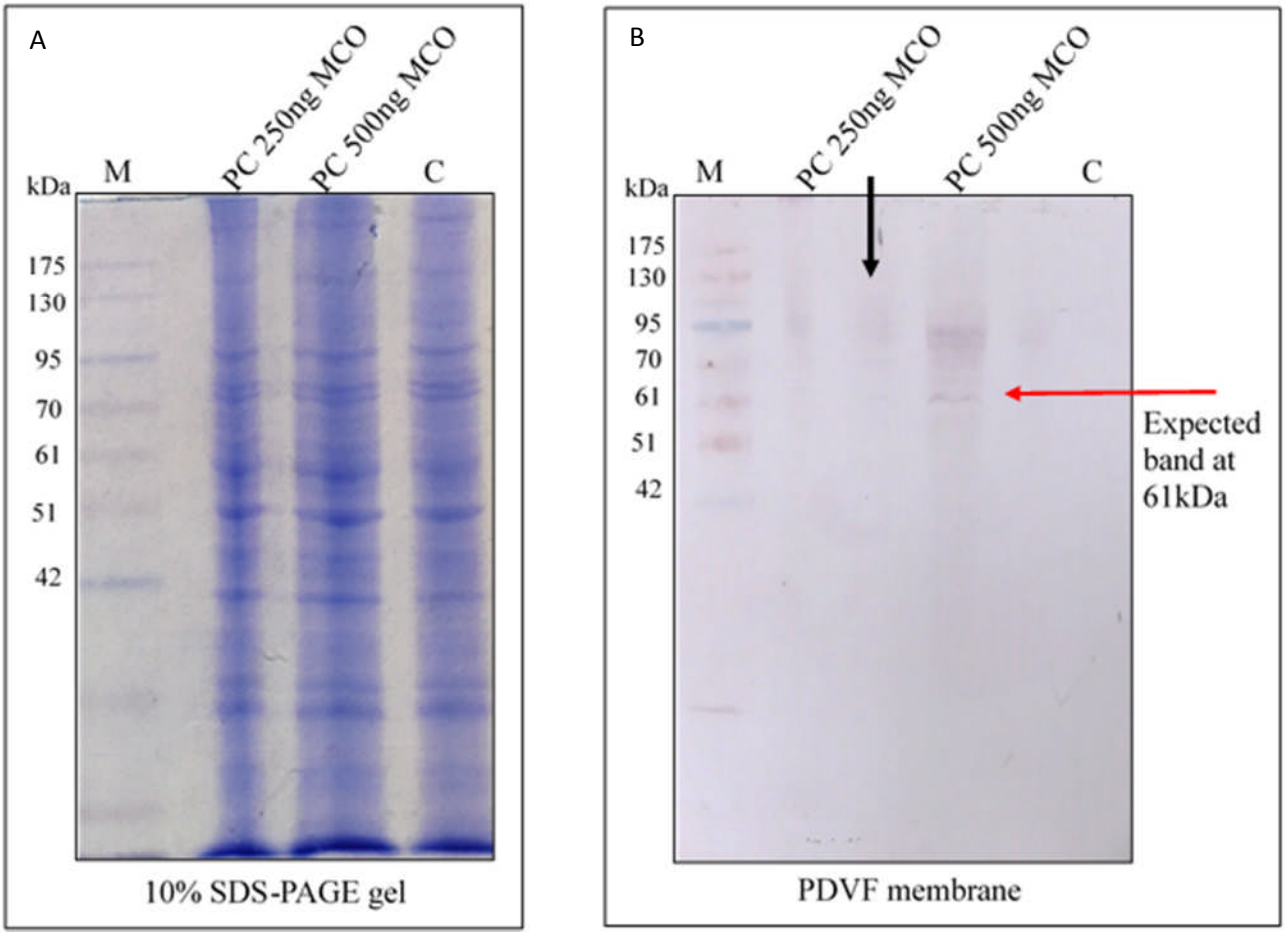

Figure 16: Confirmation of permeabilization of THP-1 cells treated with MmcO: (A) 10% SDS-PAGE gel stained by Coomassie stain represents cytoplasmic extract of the THP-1 cell permeabilized with 250 ng MmcO (PC 250 ng MmcO) fraction and cytoplasmic extract of the THP-1 cell permeabilized with 500 ng MmcO (PC 500 ng MmcO) fraction. These fractions were compared to the empty THP-1 cell extract (lane C). (B) western blot for anti-his, confirms that MmcO was successfully permeabilized in the THP-1 cells using SLO and the expected band appears at 61 kDa. M=Marker

Measurement of reactive oxygen species (ROS)

The ROS assay is the last step to determine the effect of an active MmcO protein on the production of ROS. PMA inducer is commercially characterised as an inducer to promote the production of ROS. Thus, optimising the incubation time after inducing the cells with/without PMA in the presence of different MmcO protein concentrations was very important factor in this experiment. The ROS readings were conducted after 15 min and 30 min of incubation. The result shows that the highest ROS production was measured at 30 min incubation period. Based on this result, the ROS assay was incubated for 30 min before the detection stage (Figure 17). Longer time periods were also investigated but activity of MmcO was seen to decrease beyond 30 minutes (data not shown).

After the induction with PMA, the results of the ROS assay on the permeabilized cells were compared to the 0ng MmcO condition for each experiment, which was used as the negative control (Figure 18). The graph illustrates that ROS productions did not show any significant affects at certain level of MmcO (between 10 ng and 100 ng) in induced cells, whereas 250 ng of MmcO sample showed a slight increasing by 10.9%. However, the comparison between the control (0 ng) and 500ng concentrations of MmcO showed an obvious decrease in the ROS production by almost 14.1 %. Statistically, the concentrations (10 ng, 100 ng, and 250 ng) of MmcO protein did not show any statistical differences relative to the control, whereas the highest concentration (500 ng) of MmcO showed a statistical difference with p value < 0.05 to the control (Figure 18 A). The uninduced-permeabilized cells did not illustrate any ROS production differences (Figure 18 B). Moreover, the calculated ratio between induced and uninduced reactions indicated the same general results (Figure 19). In the presence of 500 ng MmcO, the ROS was reduced by 32.1% in the permeabilized THP-1 cell (Figure 19). Furthermore, testing the effect of MmcO protein outside

the cells by treating non-permeabilized induced cells with 500 ng MmcO protein showed a 19.9% decrease in the ROS production compared to the control (Figure 20 A). Statistically, the concentrations 500ng of MmcO protein showed a statistical difference with p value < 0.01 to the control. The bar graph (Figure 20 B) illustrates that there was no significant difference between results of ROS production in uninduced cells that were either exposed to MmcO or not.

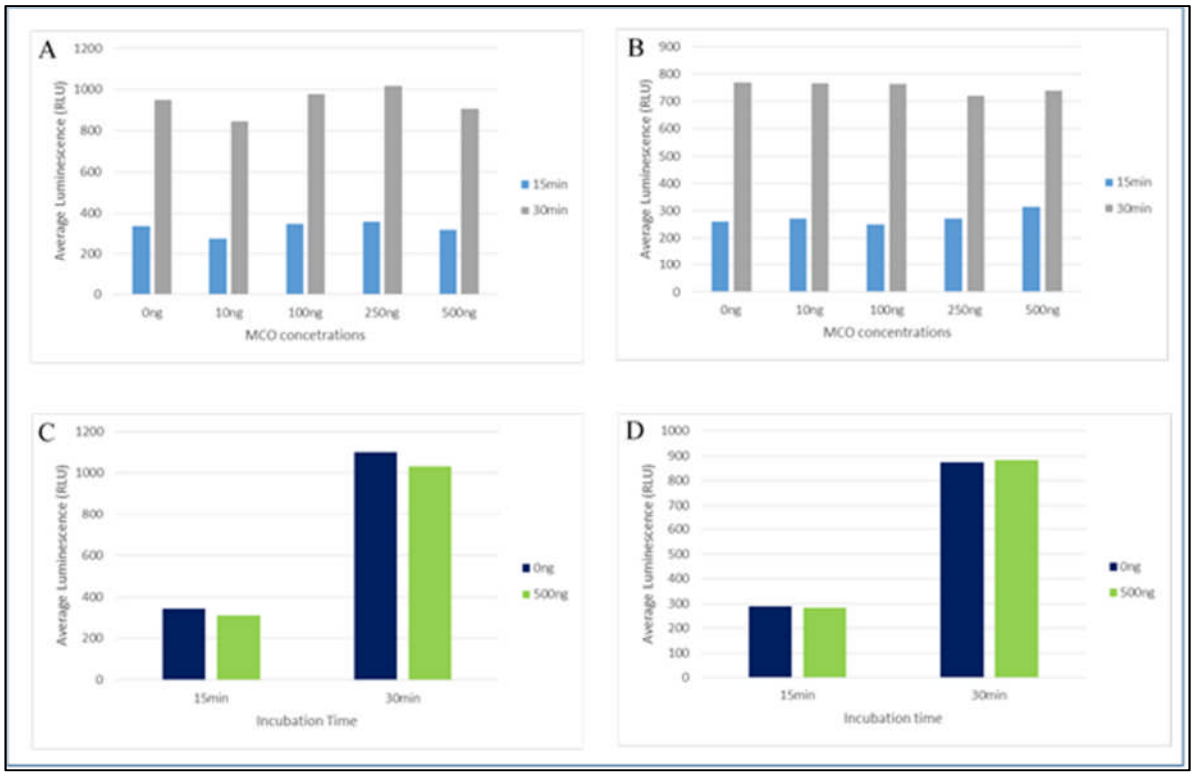

Figure 17: Optimizing the Incubation Time for the ROS Reduction by MmcO: The graphs show the average amount of ROS production in the presence of different MmcO protein concentrations, after the induction with/without PMA inducer in (15min and 30min). (A) permeabilized and induced samples, (B) permeabilised and uninduced samples. However, (C) non-delivered and induced samples, and (D) non- delivered and uninduced samples. Generally, the highest level of ROS production is presented differently between the various concentrations of MmcO after 30min of induction compared to 15min.

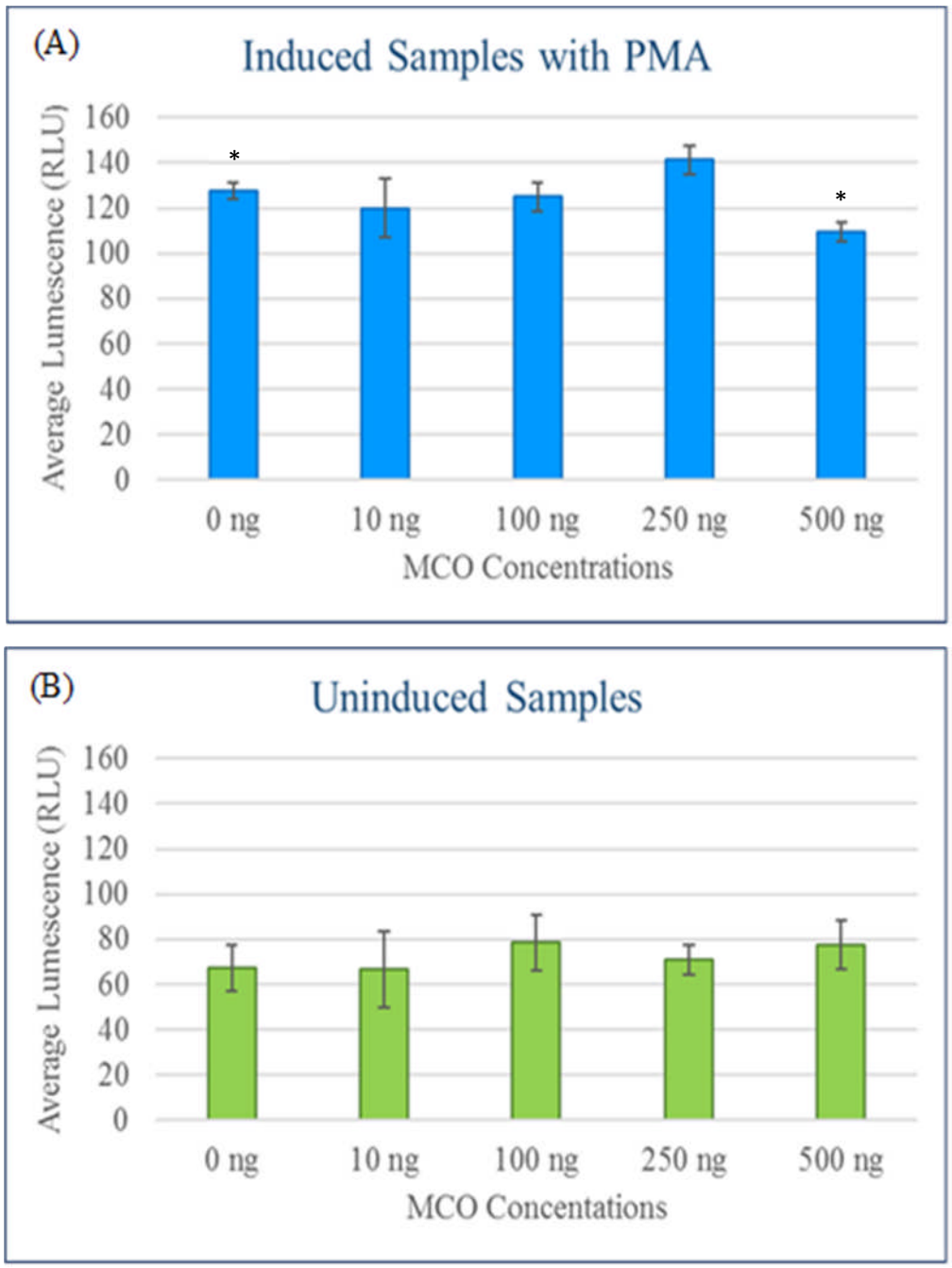

Figure 18: ROS production in permeabilized THP-1 cells treated with MmcO: The graphs illustrate the average amount of ROS production in the presence of different MmcO protein concentrations (10 ng, 100 ng, 250 ng, 500 ng) after the induction (A) with PMA inducer and (B) without PMA induction. The values are represented in both graphs as mean of three individual experiments carried out in duplicate. Bars represent the mean ± standard error. In the induced samples (A), the ROS production show a significant decrease in the production of ROS at 500 ng of MmcO comparing to 0 ng. * indicates a statistical difference in induced sample relatively to the 0ng with $p<0.05$. However, (B) graph does not show any ROS production differences comparing to the control.

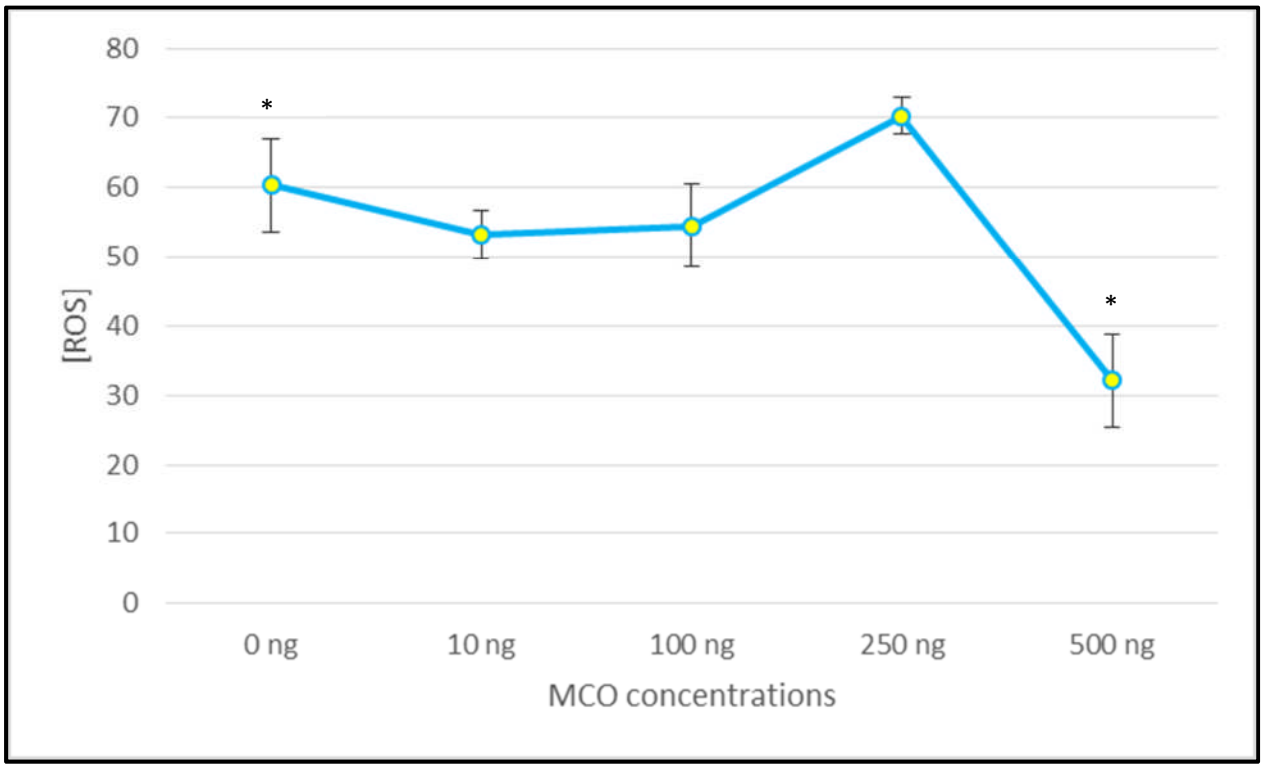

Figure 19: ROS ratio between induced and uninduced THP-1 cells with MmcO: the ratio of the ROS production represented in this graph in the different concentration of MmcO and bars indicate the mean ± standard error. From the data, there is a decrease of ROS level at 500ng of MmcO. This indicates the greatest reduction affect in the ROS production level. * indicates a statistical difference relatively to the 0ng with $p<0.05$.

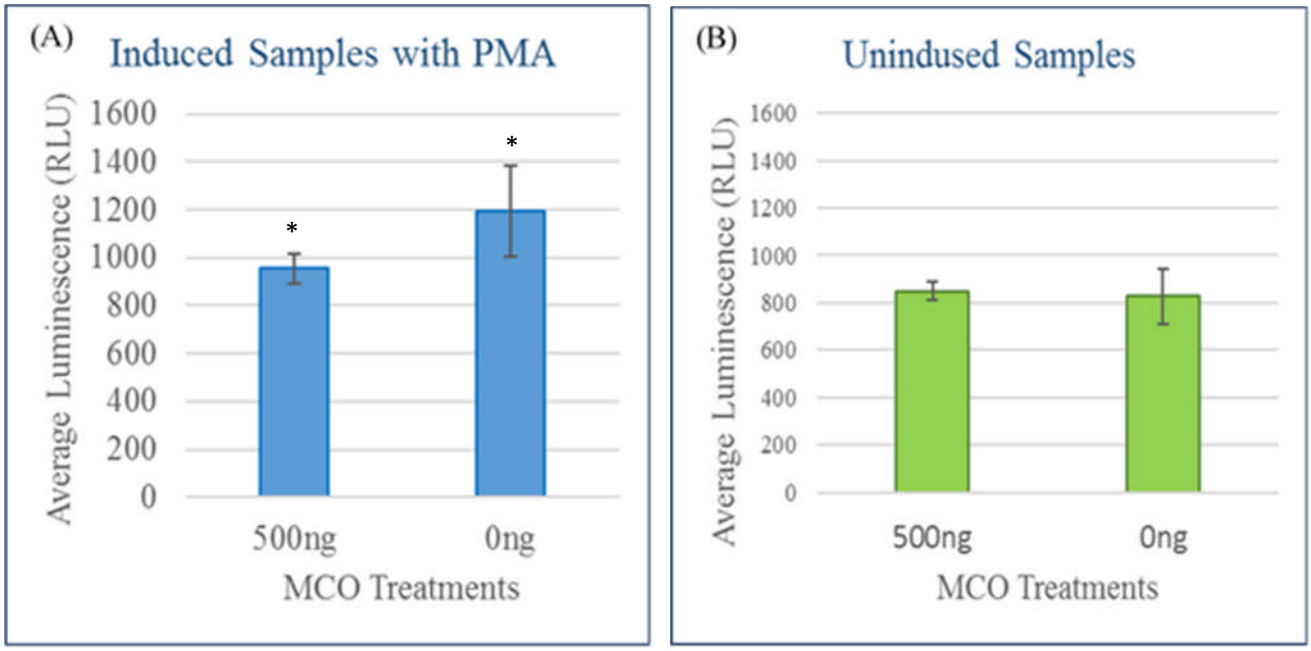

Figure 20: ROS generation in non-permeabilized THP-1 cells with MmcO: The graphs represent the average amount of ROS production in the presence of 500 ng MmcO protein concentration after the induction (A) with PMA and without PMA (B) induction. The values are represented in both graphs as mean of three individual experiments carried out in duplicate. Bars represent the mean ± standard error. (A) In induced samples, ROS production shows a significant decrease at 500 ng compared to the control (0 ng). * indicates a significant statistical difference in samples relatively to the 0ng with $p<0.01$. However, (B) graph does not show any ROS production differences compared to the control.

Discussion

Mycobacterium tuberculosis is an intracellular pathogenic bacterium that arrests the respiratory burst process during phagocytosis. *M. tuberculosis'* pathogenicity is derived from its possession of several putative virulence factors that contribute to inhibition of ROS production and phagocytosis maturation while allows it to survive in the macrophage. In this study, we investigated the impact of multi-copper oxidase (MmcO), coded by the *M. tuberculosis's* Rv0846c gene, on the production of ROS in living monocytic cells. It is known that ROS are produced in cells during phagocytosis, where they serve as a shield to protect the host from microbial attack. Several studies have shown that *M. tuberculosis* can prevent ROS mediated damage by secreting superoxide dismutase (SodC and SodA) and catalase-peroxidase (KatG) (Liao et al, 2013; Mo et al, 2004). These secreted enzymes are characterized by their oxidative activity and since *M. tuberculosis* multi-copper oxidase (MmcO) also catalyzes oxidoreductase activities, MmcO may also prevent ROS mediated damaged.

The main focus of our study is to clone, express, purify and test the contribution of active MmcO protein towards the protection of the pathogen from ROS molecules. This was done by delivering different concentrations of a purified and active MmcO protein into living THP-1 cells by utilizing Streptolysin O as a penetration tool. The THP-1 cell line can produce ROS in response to stimulation and is suitable to understand the role of MmcO during the respiratory burst process.

Cloning and Expression of the *Mycobacterium tuberculosis rv0846c* gene

Over decades, *E. coli* has been an effective host to produce recombinant proteins. The combination of its fast growth and its well-studied genetics makes *E. coli* the most suitable host

for high expression of the target recombinant protein, often producing milligram quanitites of recombinant proteins per liter (Baneyx, 1999; Rosano & Ceccarelli, 2014). The yield of the over-expressed protein may be on average of 30%-40% of total intracellular protein expression (Georgiou & Valax, 1996; Suzuki et al, 2006).

The cloning and expression of the *rv0846c* gene into the pMAL vector was first conducted in our laboratory by Johanna Delongchamp. In brief, the synthesized *rv0846c* gene from the *M. tuberculosis* H37Rv genome was obtained from GenScript in a pJET 1.2 vector. It was sub-cloned into the pMAL c5x/p5x expression vectors, and expressed in an *E. coli* NEB expression host. While the cloning was successful, the expression of the gene eventually failed. There are several possible reasons for this failure; first, pMAL harbours a cleavable maltose binding protein (MBP) sequence that tags proteins upstream the gene which allows tag cleavage after protein purification. However, N-terminal labeling was generally avoided because it may disrupt the structure of Rv0846c and interfere with MmcO protein expression. The other reason for failure appeared to be the purification failure using the amylose column; although an overexpressed protein at 96kDa, consisted with the combination of MBP (~43 kDa) and the MmcO (~54 kDa), was obtained. This led us to investigate the cloning design that was used to clone the *rv0846c* gene. This showed that the two genes were cloned with no linker which may promote improper or misfolding of the MBP binding site and lead to purification failure. The final reason for the failure could be that the misfolding of the expressed protein affected its secondary and tertiary protein structure, which disrupted the cleaving site between the MBP and MmcO and resulted in failure of Factor-X digestion to cleave the site.

To avert the challenges encountered in past experiments, the *rv0846c* gene was cloned into the pET21a expression vector that contains the His affinity tag, and transformed it into the *E. coli*

BL21 expression host. Additionally, cloning proteins of interest into a plasmid with an affinity tag facilitates the detection and purification of the recombinant proteins (Rosano & Ceccarelli, 2014). We designed primers with the addition of 9 amino acids to code for a linker between the 6x-His tag and the *rv0846c* gene to limit misfolding and keep the His-tag separated from the mature protein structure to ensure exposure of the tag for purification.

Heterologous production and purification of MmcO from inclusion bodies

In many instances when the recombinant protein is expressed in a heterologous host, protein degradation, a low expression level, aggregation of proteins, or insolubility may result (Georgiou & Valax, 1996). On the other hand, a high level or over-expression of recombinant protein in the host cell, together with the lack of an adequate amount of chaperones, and high concentration of folding intermediates, can result in the formation of insoluble structures called inclusion bodies (Palmer & Wingfield, 2004). The aggregated proteins of the inclusion bodies are biologically inactive although they can be up to 40-90% pure for a single protein and offer protection from proteases (Georgiou & Valax, 1996). The predicted localization of the expressed MmcO protein was in the periplasmic space but tethered to the cytoplasmic membrane by lipidation of cysteine at position 35. However, protein electrophoresis and western blot analysis (See Figure 11A, B) did not show a distinct band at ~61kDa in the two periplasmic or cytoplasmic fractions. Instead, a high-intensity band of about ~61kDa in size, in the insoluble fraction (inclusion bodies) was obtained (Figure 11A). This result confirmed previous studies by Rowland and Niederweis (2013) who showed that MmcO protein expressed in *E. coli* BL21 and was presented in inclusion bodies. Several strategies by the authors, including various fusions, to express a properly folded and functional MmcO were unsuccessful. This result was confirmed by

western blot analysis of all fractions (except WC fraction) with an anti-6xHis antibodies (See Figure 11 B "SDS-PAGE"). The targeted band at ~61 kDa was present in the blot which suggested the MmcO protein is in fact insoluble but was successfully expressed. Over expression resulted in inclusion bodies regardless of the presence of the MmcO signal peptide (See Figure 11 B "PVDF membrane").

The MmcO protein was extracted from inclusion bodies using the method of Rudolph & Lilie (1996) with some modifications. The idea was to obtain functional MmcO by refolding of the denatured protein. However, in vitro, this approach may result in polypeptide misfolding and aggregation (Tsumoto et al, 2003). To overcome this, urea was gradually reduced to a low concentration by step-wise dialysis. This resulted in successful and proper MmcO protein folding (Figure 12 A PC). The refolded MmcO was a large majority of the aggregated protein and was relatively pure as demonstrated on 10% SDS-PAGE which showed double bands; one of them was at the right size for MmcO protein (61kDa). In order to get a highly purified MmcO protein, nickel affinity chromatography was used. The purification process was done in two stages. In the first stage, the refolding buffer was exchanged with a conditioning buffer that contains a low concentration of imidazole (20mM). The conditioning buffer was used to keep MmcO in a buffer compatible with the nickel affinity resin, and to increase the affinity of the His-tag for the nickel resin and minimize nonselective binding of host proteins. The SDS-PAGE results showed a single band which suggests the elution was not contaminated with a significant amount of non-specific proteins (Figure 12A P-MmcO). The purified MmcO protein could be resolved on SDS-PAGE as a single band at about 61kDa and the PVDF membrane confirmed presence of the His tag (Figure12 A&B P-MmcO).

Enzyme activity of MmcO

The substrate 2,2-azino-bis (3-ethylbenzothiazoline-6-sulphonic acid), or ABTS, was used to characterize the enzymatic activity of the purified MmcO protein. When the purified MmcO enzyme was combined with the ABTS, the reaction produced a soluble green-colored product. Contrary to a recent study that maintained a 5-minute monitoring of the MmcO activity (Rowland & Niederweis, 2013), we found that a 5-minute incubation time is insufficient. Monitoring the absorbance for the color change of ABTS every 30 min for four hours revealed that after the first 30 minutes, a 20 µg (0.33nmol) sample of the MmcO had a consistent high activity translating to about 47 nmol/min.mg protein. During the following intervals, there was a gradual decrease such that at the fourth hour mark, there was less than 10 nmol/min.mg (See Figure 13). This level of specific activity translates to 235 $\mu M \cdot min^{-1} \cdot mg^{-1}$. This is considered substantial activity considering that lysates of wild type *M. tuberculosis* show activities towards ABTS in the range of 2 $\mu M \cdot min^{1} \cdot mg^{1}$ (Rowland and Niederweis, 2013). Although the gels and the western blots in this study show a single band for the purified MmcO such data does not exclude the presence of denatured protein in the samples. Further analysis using analytical gel permeation or sedimentation experiments will need to be crried out to establish how much of the purified and refolded protein is in fact properly folded.

***M. tuberculosis'* MmcO may potentially suppress the production of ROS**

Reactive Oxygen Species (ROS) for example, superoxide, oxygen ion, and H_2O_2, are extremely reactive molecules (Newsholme et al, 2012). They are continuously produced in the process of macrophage phagocytosis as a macrophage antibacterial method. However, when they

produced in excess amounts, they can lead to oxidation of proteins and DNA, in addition to cross-liking proteins and degrade pathogenic bacteria (Uy, McGlashan, & Shaikh, 2011).

To address the last aim of this study, it was important for us to study the impact of MmcO on ROS generated within cells (Uy, McGlashan & Shaikh, 2011). THP-1 cells, a human monocyte leukemia cell line (Adati et al, 2009), were used to investigate ROS production and effects of MmcO thereon. Purified MmcO was added to the THP-1 cells using Streptolysin O to facilitate membrane permeability following the Walev et al. (2010) protocol. THP-1 cells were chosen because it is one of macrophage lineages (Uy, McGlashan, & Shaikh, 2011) and can generate ROS to model the production of ROS by monocyte/macrophages during their immune pathway response (Chanputa et al, 2014). The THP-1 cells were treated with Phorbol 12-myristate 13-acetate (PMA) to promote the ROS production (Uy, McGlashan, & Shaikh, 2011).

In vitro, hydrogen peroxide (H_2O_2) produced by the THP-1 cell line is a useful read out of the ROS (Newsholme et al, 2012). H_2O_2 has a longer life in solution and can easily diffuse from the cell, thus proving to be an excellent oxidation stress marker (Duellman et al, 2013). In order to test the theory that MmcO protein can reduce the amount of ROS, we measured the H_2O_2 produced by THP-1 cells, treated with MmcO and afterword with PMA. First, Optimizing the incubation duration was very important factor in this experiment. Thus, we carried the optimization experiment up with an interval of 15 and 30 minutes to enable us to optimize the time of the reaction. It is evident that MmcO showed its activity against ROS after 30 minutes period of the reaction, which was also compatible with the highest MmcO activity read against ABTS (See Figure 17). Based on this result, the ROS-Glo Assay kit was incubated for about 30 minutes on the permeabilized THP-1 cells that were treated with several concentrations of the MmcO protein (10 ng, 100 ng, 250 ng, 500 ng) and compered to the control (0 ng of MmcO). It was said that

several ROS are usually converted to H_2O_2 in a cell and because H_2O_2 half-life is long enough, any increase in the H_2O_2 shows a relative increase in the levels of ROS. The chemical pathway for ROS-Glo assay was started by using a H_2O_2 substrate that directly reacted with H_2O_2 to produce Luciferin precursor, which was not an appropriate substrate for use by luciferase. By adding the ROS-Glo Detection Solution, the precursor was converted to luciferin, which made it possible for luciferase and other compounds to be able to produce light signals that were equivalent to the present H_2O_2 levels (See Figure 7) (Duellman et al, 2013).

Interestingly, we found that when we exposed the induced/uninduced THP-1 cells to the 500 ng purified MmcO, the levels of ROS were reduced. On the other hand, ROS production did not indicate a significant increased when treated with 10ng and 100ng of MmcO, but there was a slight increase in ROS production at 250ng of MmcO (Figure 18 A). However, this increase did not indicate any statistical difference comparing to the control. The 500ng showed an obvious statistical difference with p value < 0.05 relatively to the control; therefore, we hypothesised that the reduction of ROS levels in the presence of higher level of MmcO (500ng) could be due to several reasons. First, the 500ng of MmcO protein may have contained just the right fraction of active enzyme to effect further ROS production. Second, since ROS being inducible in the experiment, its production would be less likely to be affected from the low MmcO protein concentration whereas 500 ng of MmcO protein was enough to show an effective detectable shift on the ROS production because the enzyme needed to be active during the experiment. Finally, any level of MmcO, when used intracellularly, may have shorter half-life where intracellular factors including proteases may have made it impossible for the low levels of MmcO to cause a detectable reduction in ROS levels. However, the assay mechanism is based on measuring all the ROS production in the reaction volume (in- and outside the cell). Therefore, the slight increase of

the ROS production at 250 ng of MmcO might be a result of the outside ROS measurement, since ROS such as H_2O_2 can be easily defused across the cytoplasmic membrane to outside the cell when MmcO was restricted to the ROS inside the cell. Another theory could be some undetectable *E. coli* proteins residual accompanied MmcO during the purification, enhanced the production of ROS along with PMA inducer. Our calculations of the ROS concentration ratio between the induced/uninduced cells confirmed that the effect of 500 ng MmcO protein was to reduce the ROS concentration by 32.1 % as compared to other concentrations (Figure 19). Additionally, the impact of 500 ng MmcO protein on extracellular ROS production was tested and shown to be very efficient and statistically difference with p value < 0.01 relatively to the control (Figure 20 A). The most likely reason for this observation is that MmcO could be used as scavenger outside cells by interfering with the ROS molecules production through reduction of levels of available oxygen. Since the MmcO is from the same family as the Laccases, it is possible that it may have similar impacts on oxidizing host substances to produce scavengers of reactive species and maintain a reducing environment for pathogens (Zhu et al, 2001). Nevertheless, extracellular laccases, if present, reduce free ions in the macrophage and prevents respiratory burst responses (Zhu et al, 2001). Our experiments showed unanticipated results where the uninduced and non-permeabilized THP-1 cells showed a high level of ROS production even though they were not exposed to PMA inducer (Figure 20 B). A possible explanation for this outcome would be that even though ROS production is PMA controlled, there is always some ROS production by any environmental substances including LPS, or the natural ROS production from the cell's organelles. Collectively, these may have contributed heavily to the observed levels of ROS. Additionally, treatment of the cell with SLO and permeabilization of the membrane may render the cells more sensitive or

responsive to environmental stress than non-permeabilized cells. Conversely, treated cells may experience disturbance in their ability to respond effectively to environmental stimuli.

Conclusion

The main goal of this study was to explore a possible role for a purified and active *M. tuberculosis rv0846c* gene product, MmcO, in interfering with ROS production in model macrophages. The MmcO protein was extracted from inclusion bodies and refolded into an active form. To date, it is the first report of functional recombinant MmcO. Recombinant MmcO suppressed ROS levels in THP-1 cells. This effect was observed when the MmcO protein was delivered inside THP-1 cells via membrane permeabilization with Streptolysin O or when used outside the cells.

Bibliography

Achard, M. E., Tree, J. J., Holden, J. A., Simpfendorfer, K. R., Wijburg, O. L., Strugnell, R. A., Schembri, M. A., Sweet, M. J., Jennings, M. P. & McEwan, A.G. (2010). The Multi-Copper-Ion Oxidase CueO of Salmonella enterica Serovar Typhimurium is Required for Systemic Virulence. *Infect. Immun., 78* (5): 2312– 2319.

Adati, N., Huang, M. C., Suzuki, T., Suzuki, H. & Kojima, T. (2009). High-Resolution Analysis of Aberrant Regions in Autosomal Chromosomes in Human Leukemia THP-1 Cell Line. *BMC Research Notes, 2* (153): 1-7.

Armstrong, J. A. & Hart, P. D. (1975). Phagosome-lysosome Interactions in Cultured Macrophages Infected with Virulent Tubercle Bacilli. *The Journal of Experimental Medicine, 142*: 1-15.

Balasubramanian, R. & Rosenzweig, A.C. (2007). Structural and Mechanistic Insights into Methane Oxidation by Particulate Methane Monooxygenase. *Acc Chem Res, 40* (7): 573-580.

Baneyx, F. (1999). Recombinant Protein Expression in *Escherichia coli*. *Curr Opin Biotechnol. 10*(5):411-21.

Berg, J. M., Tymoczko, J. L. & Stryer, L. (2002). *Biochemistry. 5th edition*: *Section 4.1The Purification of Proteins Is an Essential First Step in Understanding Their Function.* New York, USA: W H Freeman.

Berton, G., Cassatella, M. A., Bellavite, P. & Rossi, F. (1986). Molecular Basis of Macrophage Activation. Expression of the Low Potential Cytochrome b and Its Reduction upon Cell Stimulation in Activated Macrophages. *J Immunol., 136*(4):1393-9.

Boshoff, H. I. & Barry, C. E. (2005). Tuberculosis - Metabolism and Respiration in the Absence of Growth. *Nat Rev Microbiol 3* (1): 70–80.

Bourbonnais, R., Leech, D. & Paice, M. G. (1998). Electrochemical Analysis of the Interactions of Laccase Mediators with Lignin Model Compounds. *Biochimica et Biophysica Acta 1379*:381–390.

Cambier, C. J., Falkow, S. & Ramakrishnan, L. (2014). Host Evasion and Exploitation Schemes of Mycobacterium Tuberculosis. *Cell 159* (7): 1497–1509.

Centers for Disease Control and Prevention. (2016). *Treatment for TB Disease*.

http://www.cdc.gov/tb/topic/treatment/tbdisease.htm

Centers for Disease Control and Prevention. (2016). *Tuberculosis (TB) Disease: symptoms & Risk Factors.* http://www.cdc.gov/features/tbsymptoms/

Cha, J. S. & Cooksey, D. A. (1991). Copper Resistance in *Pseudomonas syringae* Mediated by Periplasmic and Outer Membrane Proteins. *Proc. Natl. Acad. Sci. U. S. A. 88* (20): 8915–8919.

Chanputa, W., Mesb, J. J. & Wichersb, H. J. (2014). THP-1 Cell Line: An in Vitro Cell Model for Approach. Immune Modulation. *International Immunopharmacology, 23* (1): 37–45.

Cole, S. T., Brosch, R., Parkhill, J., Garnier, T., Churcher, C., Harris, D., Gordon, S. V., et al. (1998). Deciphering the Biology of Mycobacterium Tuberculosis from the Complete Genome Sequence. *Nature 393* (6685): 537–44.

Comas, I., Coscolla, M., Luo, T., Borrell, S., Holt, K. E., et al. (2013). Out-of-Africa Migration and Neolithic Co-Expansion of *Mycobacterium tuberculosis* with Modern Humans. *Nat Genet., 45*(10): 1176–1182.

Crichton, R. R. & Pierre, J. L. (2001). Old Iron, Young Copper: from Mars to Venus. *Biometals, 14* (2): 99-112.

Cross, A. R. & Segal, A. W. (2004). The NADPH Oxidase of Professional Phagocytes-Prototype of the NOX Electron Transport Chain Systems. *Biochim Biophys Acta, 1647* (1): 1-22.

Daffé, M. & Draper, P. (1998). The Envelope Layers of Mycobacteria with Reference to their Pathogenicity. *Adv Microb Physiol., 39*:131-203.

Dahlgren, C. & Karlsson, A. (1999). Respiratory Burst in Human Neutrophils. *Journal of Immunological Methods, 232* (1-2): 3–14.

Daniel, T. M. (2006). The History of Tuberculosis. *Respiratory Medicine, 100* (11): 1862–70.

Dwivedi, R. (2011). *Civil Services Prelims Paper I 60 Days*. New York, USA: Tata McGraw Hill Education Private Limited.

Deffert, C., Cachat, J. & Krause, K. (2014). Phagocyte NADPH Oxidase, Chronic Granulomatous Disease and Mycobacterial Infections. *Cellular Microbiology, 16* (8): 1168–1178.

Duellman, S., Shultz, J., Vidugiris, G. & Cali, J. (2013). A New Luminescent Assay for Detection of Reactive Oxygen Species. *Promega Corporation*, 1-9.

Ehrt, S. & Schnappinger, D. (2009). Mycobacterial Survival Strategies in the Phagosome:

Defense Against Host Stresses. *Cell Microbiol*, *11*(8): 1170–1178.

Forrellad, M. A., Klepp, L. I., Gioffré, A., García, J. S. y, Morbidoni, H. R., et al. (2013). Virulence Factors of the *Mycobacterium tuberculosis* Complex. *Virulence 4* (1): 3–66.

Fu, L. M. & Fu-Liu, C. S. (2002). Is *Mycobacterium tuberculosis* a Closer Relative to Gram-Positive or Gram– Negative Bacterial Pathogens? *Tuberculosis, 82* (2/3): 85–90.

Gaetke, L. M. & Chow, C. K. (2003). Copper Toxicity, Oxidative Stress, and Antioxidant Nutrients. *Toxicology 189*: 147-163.

Galagan, J. E. (2014). Genomic Insights into Tuberculosis. *Nature Reviews Genetics, 15*: 307–320.

Georgiou, G. & Valex, P. (1996). Expression of Correctly Folded Proteins in *Escherichia coli. Curr Opin Biotechnol. 7*(2):190-7.

GEHealthcareBio-SciencesAB (2012). HisTrap excel (1and5ml). www.gelifesciences.com/protein-purification.

Grass, G. & Rensing, C. (2001). CueO is a Multi-copper Oxidase that Confers Copper Tolerance in *Escherichia coli*. *Biochem. Biophys. Res. Commun., 286* (5): 902– 908.

Grass, G., Rensing, C., & Solioz, M. (2011). Metallic Copper as an Antimicrobial Surface. *Appl Environ Microbiol, 77*(5): 1541-1547.

Hames, B. D. (1998). *Gel Electrophoresis of Protein: a Practical Approach* [Third Edition]. Oxford University Press, UK.

Hett, E. C. & Rubin, E. J. (2008). Bacterial Growth and Cell Division: A Mycobacterial Perspective. *Microbiol. Mol. Biol. Rev., 72* (1): 126–156.

Heppner, D. E., Kjaergaard, C. H. & Solomon, E. I. (2014). Mechanism of the Reduction of the Native Intermediate in the Multicopper Oxidases: Insights into Rapid Intramolecular Electron Transfer in Turnover. *J. Am. Chem. Soc., 136*: 17788−17801.

Hoffmann, A. & Roeder, R. G. (1991). Purification of His-Tagged Proteins in Non-Denaturing Conditions Suggests a Convenient Method for Protein Interaction Studies. *Nucleic Acids Research , 19*(22): 6337-6338.

Hsiao, Y. M., Liu, Y. F., Lee, P. Y., Hsu, P. C., Tseng, S. Y. & Pan, Y. C. (2011). Functional Characterization of CopA Gene Encoding Multicopper Oxidase in Xanthomonas campestris pv. campestris. *J. Agric. Food Chem. 59* (17): 9290– 9302.

Kang, P. B., Azad, A. K., Torrelles, J. B., Kaufman, T. M., Beharka, A., Tibesar, E., DesJardin,

L. E. & Schlesinger, L. S. (2005). The human Macrophage Mannose Receptor Directs *Mycobacterium tuberculosis* Lipoarabinomannan-mediated Phagosome Biogenesis. *JEM, 202*(7):987–999.

Kaufmann, S. H. E. (2001). How can immunology contribute to the control of tuberculosis? *Nature Reviews Immunology, 1*: 20-30.

Keshavjee, S. & Farmer, P. E. (2012). Tuberculosis, Drug Resistance, and the History of Modern Medicine. *N Engl J Med 367* (10): 931–936.

Kettle, A. J. & Winterbourn, C. C. (1990). Superoxide Enhances Hypochlorous Acid Production by Stimulated Human Neutrophils. *Biochim Biophys Acta, 1052*(3):379-85.

Klann, A. G., Belanger, A. E., Mello, A. A., Lee, J. Y. & Hatfull, G. F. (1998). Characterization of the dnaG Locus in *Mycobacterium smegmatis* Reveals Linkage of DNA Replication and Cell Division. *Journal of Bacteriology, 180*(1):65-72.

Kleinnijenhuis, J., Oosting, M., Joosten, L. A. B., Netea, M. G. & Crevel, R. V. (2011). Innate Immune Recognition of *Mycobacterium tuberculosis*. *Clinical and Developmental Immunology 2011*: 1–12.

Lakey, D. L., Voladri, R. K. R., Edwards, K. M., Hager, C., Samten, B., Wallis, R. S., Barnes, P. F. & Kernodle, D. S. (2000). Enhanced Production of Recombinant *Mycobacterium tuberculosis* Antigens in *Escherichia coli* by Replacement of Low-Usage Codons. *Infect Immun, 68*(1): 233–238.

Liao, D., Fan, Q. & Bao, L. (2013). The Role of Superoxide Dismutase in the Survival of *Mycobacterium tuberculosis* in Macrophages. *Japanese Journal of Infectious Diseases 66* (6): 480–488.

Lin, C. H., Lin, C. J., Kuo, Y. W., Wang, J. Y., Hsu, C. L., Chen, J. M., Cheng, W. C. & Lee, L. N. (2014). Tuberculosis Mortality: Patient Characteristics and Causes. *BMC Infectious Diseases, 14*(5):1-8.

Linder, M.C. & Hazegh-Azam, M. (1996). Copper biochemistry and molecular biology. *Am J Clin Nutr 63*(5): 797S-811S.

Lory, S. (2014). 29 The Family Mycobacteriaceae. *Springer-Verlag Berlin Heidelberg*, 571-575.

Mahmood T. & Yang P. (2012). Western Blot: Technique, Theory, and Trouble Shooting. *N Am J Med Sci., 4*(9): 429–434.

McDonough, J. A., McCann, J. R., Tekippe, E. M., Silverman, J. S., Rigel, N. W., & Braunstein, M. (2008). Identification of functional Tat signal sequences in Mycobacterium tuberculosis proteins. Journal of bacteriology, 190(19), 6428-6438.

Mo, L., Zhang, W., Wang, J., Weng, X. H., Chen, S., Shao, L.Y., Pang, M. Y. & Chen, Z.W. (2010). Three-Dimensional Model and Molecular Mechanism of *Mycobacterium tuberculosis* Catalase-Peroxidase (KatG) and Isoniazid-Resistant KatG Mutants. *Microb Drug Resist,10*(4): 269–279.

More, S. S., Renuka, P.S., Pruthvi, K., Swetha, M., Malini, S. & Veena, S.M. (2011). Isolation, Purification, and Characterization of Fungal Laccase from *Pleurotus sp. Enzyme Research, 2011*:1-7.

Murray, A. (2016). Salvador Luria and Max Delbrück on Random Mutation and Fluctuation Tests. *GENETICS, 202*: (2) 367-368.

Newsholme, P., Rebelato, E., Abdulkader, F., Krause, M., Carpinelli, A. & Curi, R. (2012). Reactive Oxygen and Nitrogen Species Generation, Antioxidant Defenses, and β-cell Function: a Critical Role for Amino Acids. *J Endocrinol., 214*(1):11-20.

Ng, V. H., Cox, J. S., Sousa, A. O., MacMicking, J. D. & McKinney, J. D. (2004). Role of KatG Catalase-Peroxidase in Mycobacterial Pathogenisis: Countering the Phagocyte Oxidative Burst. *Molecular Microbiology 52* (5): 1291–1302.

Niki, M., Suzukawa, M., Akashi, S., Nagai, H., Ohta, K., Inoue, M., Niki, M., et al. (2015). Evaluation of Humoral Immunity to *Mycobacterium tuberculosis*-Specific Antigens for Correlation with Clinical Status and Effective Vaccine Development. *Journal of Immunology Research 2015* (11): 1–13.

Palmer, I. & Wingfield, P. T. (2004). Preparation and Extraction of Insoluble (Inclusion-Body) Proteins from *Escherichia coli. Curr Protoc Protein Sci., Chapter unit-6.3.:*1-25.

Pena, M. M., Lee, J. & Thiele, D.J. (1999). A Delicate Balance: Homeostatic Control of Copper Uptake and Distribution. *J Nutr, 129*(7): 1251-1260.

Pethe, K., Swenson, D. L., Alonso, S., Anderson, J., Wang, C. & Russell, D. G. (2004). Isolation of *Mycobacterium tuberculosis* Mutants Defective in the Arrest of Phagosome Maturation. *The National Academy of Sciences of the U S A, 101* (37): 13642–13647.

Piddington, D. L., Fang, F. C., Laessig, T., Cooper, A. M., Orme, I. M. & Buchmeier, N. A. (2001). Cu, Zn Superoxide Dismutase of *Mycobacterium tuberculosis* Contributes to

Survival in Activated Macrophages that are Generating an Oxidative Burst. *Infect Immun, 69* (8): 4980-4987.

Prozorov, A. A., Fedorova, I. A., Bekker, O. B. & Danilenko, V. N. (2014). The Virulence Factors of *Mycobacterium tuberculosis*: Genetic Control, New Conceptions. *Russian Journal of Genetics, 50* (8): 775–797.

Poyart, C., Pellegrini, E., Gaillot, O., Baptista, M., Trieu-cuot, P. & Boumaila, C. (2001). Contribution of Mn-Cofactored Superoxide Dismutase (SodA) to the Virulence of Streptococcus Agalactiae Contribution of Mn-Cofactored Superoxide Dismutase (SodA) to the Virulence of *Streptococcus agalactiae*. *Infection and Immunity, 69* (8): 5098–5106.

Raina, H., Bhat, A., Bhat, F. A., Changal, K. H., Dhobi, G. N., Koul, P. A., Raina, M. A., Wani, F. A. (2013). Pulmonary Tuberculosis Presenting with Acute Respiratory Distress Syndrome (ARDS): A Case Report and Review of Literature. *Egyptian Journal of Chest Diseases and Tuberculosis, 62*: 655–659.

Rayhman, M., Sjaastad, M. D. & Falkow, S. (1996). Acidification of Phagosomes Containing *Salmonella typhimurium* in Murine Macrophages. *Infect Immun, 64* (7): 2765-73.

Rosano, G. L. & Ceccarelli, E. A. (2014). Recombinant Protein Expression in *Escherichia coli*: Advances and Challenges. *Front Microbiol., 5*:172.

Rowland, J. L. & Niederweis, M. (2013). A Multicopper Oxidase Is Required for Copper Resistance in *Mycobacterium tuberculosis*. *J Bacteriol. 195*(16): 3724–3733.

Rudolph, R. & Lilie, H. (1996). In Vitro Refolding of Inclusion Body Proteins. *Faseb J,10*: 49–56.

Quintanar, L., Stoj, C., Taylor, A. B., Hart, P. J., Kosman, D. J. & Solomon, E. I. (2007). Shall We Dance? How a Multicopper Oxidase Chooses Its Electron Transfer Partner. *Acc. Chem. Res., 40* (6): 445–452.

Sakamoto, K. (2012). The Pathology of *Mycobacterium tuberculosis* Infection. *Veterinary Pathology, 49* (3): 423-439.

Saviola, B. (2013). *Mycobacterium tuberculosis* Adaptation to Survival in a Human Host. *Tuberculosis - Current Issues in Diagnosis and Management,* 3–18.

Seres, T., Knickelbein, R. G., Warshaw, J. B. & Johnston, R. B. (2000). The Phagocytosis-Associated Respiratory Burst in Human Monocytes Is Associated with Increased Uptake of Glutathione. *Journal of Immunology, 165* (6): 3333-3340.

Shi, L., Sohaskey, C. D., Kana, B. D., Dawes, S., North, R. J., Mizrahi, V., & Gennaro, M. L. (2005). Changes in Energy Metabolism of *Mycobacterium tuberculosis* in Mouse Lung and Under in Vitro Conditions Affecting Aerobic Respiration. *Proc Natl Acad Sci U S A, 102* (43): 15629-15634.

Shi, X. & Darwin K. H. (2015). Copper Homeostasis in *Mycobacterium tuberculosis. Metallomics, 7* (6): 929–934.

Smith, I. (2003). *Mycobacterium tuberculosis* Pathogenesis and Molecular Determinants of Virulence. *Clinical Microbiology Reviews 16* (3): 463–496.

Solomon, E. I., Sundaram, U. M. & Machonkin, T. E. (1996). Multicopper Oxidases and Oxygenases. *Chem. Rev. 96* (7): 2563-2606.

Sturgill-Koszycki, S., Schlesinger, P. H., Chakraborty, P., Haddix, P. L., Collins, H. L., et al. (1994). Lack of Acidification in Mycobacterium Phagosomes Produced by Exclusion of the Vesicular Proton-ATPase. *Science, 263* (5147): 678-681.

Suzuki, M., Roy, R., Zheng, H., Woychik, N. & Inouye, M. (2006). Bacterial Bioreactors for High Yield Production of Recombinant Protein. *J Biol Chem., 281*(49):37559-65.

Tan, S. & Russell, D. G. (2015). Trans-Species Communication in the *Mycobacterium tuberculosis*- Infected Macrophage. *Immunological Reviews, 264*(5): 233–248.

Thermo Scientific ABTS Substrates. Fisher Scientific manual product. https://www.fishersci.ca/shop/products/pierce-abts-substrates/p-4532138

Tsuchiya, S., Yamabe, M., Yamaguchi, Y., Kobayashi, Y., Konno, T. & Tada, K. (1980). Establishment and Characterization of a Human Acute Monocytic Leukemia Cell Line (THP-1). *IJC, 26* (2): 171–176.

Tsumoto, K., Ejima, D., Kumagai, I. & Arakawa, T. (2003). Practical Considerations in Refolding Proteins from Inclusion Bodies. *Protein Expr Purif., 28*(1):1-8.

Uy, B., McGlashan, S. R. & Shaikh, S. B. (2011). Measurement of Reactive Oxygen Species in the Culture Media Using Acridan Lumigen PS-3 Assay. *Journal of Biomolecular Techniques 22* (3):95–107.

Verver, S., Warren, R. M., Beyers, N., Richardson, M., Van Der Spuy, G. D., et al. (2005). Rate of Reinfection Tuberculosis after Successful Treatment Is Higher than Rate of New Tuberculosis. *American Journal of Respiratory and Critical Care Medicine 171* (12): 1430–1435.

Wagner, D., Maser, J., Lai, B., Cai, Z., Barry, C. E. 3rd, Honer Zu Bentrup, K., Russell, D. G. & Bermudez, L. E. (2005). Elemental Analysis of *Mycobacterium avium*-, *Mycobacterium tuberculosis*-,and*Mycobacterium smegmatis*-Containing Phagosomes Indicates Pathogen-Induced Microenvironments within the Host Cell's Endosomal System. *J Immunol, 174*(3):1491-500.

Walev, I., Bhakdi, S. C., Hofmann, F., Djonder, N., Valeva, A., Aktories, K. & Bhakdi, S. (2001). Delivery of Proteins into Living Cells by Reversible Membrane Permeabilization with Streptolysin-O. *PNAS, 98*(6):3185–3190.

White, C., Lee, J., Kambe, T., Fritsche, K. & Petris, M. J. (2009). A Role for the ATP7A Copper-Transporting ATPase in Macrophage Bactericidal Activity. *J Biol Chem, 284*(49): 33949-33956.

Weiss, G. & Schaible, U. E. (2015). Macrophage Defense Mechanisms against Intracellular Bacteria. *Immunological Reviews 264* (1): 182–203.

World Health Organisation. (2014). *WHO Global Tuberculosis Report.* http://apps.who.int/iris/bitstream/10665/137094/1/9789241564809_eng.pdf

World Health Organisation. (2015). *Tuberculosis vaccine development.* http://www.who.int/immunization/research/development/tuberculosis/en/

World Health Organisation. (2015). *WHO Global Tuberculosis Report.* file:///C:/Users/Tina/Desktop/New%20folder/April%2015,16/gtbr2015_executive_summary.pdf

World Health Organisation. (2016). *WHO Tuberculosis Fact sheet N°104*. http://www.who.int/mediacentre/factsheets/fs104/en/

Zhu, X., Gibbons, J., Garcia-Rivera, J., Casadevall, A. & Williamson, P. R. (2001). Laccase of Cryptococcus neoformans Is a Cell Wall-Associated Virulence Factor. Infect. *Immun. September, 69*(9): 5589-5596.

Appendix

The Rv0846c amino acid Sequence from *M. tuberculosis* H37Rv using TubercuList:

Gene name: Rv0846c.

Function: May have multicopper oxidase activity.

Product: Probable oxidase.

Protein MW: 53795.9 Da.

Protein length: 504 aa.

Amino acid composition: A54 C2 D33 E16 F13 G55 H18 I28 K12 L38 M17 N19 P41 Q11 R26 S19 T47 V32 W7 Y16.

MPELATSGNA FDKRRFSRRG FLGAGIASGF ALAACASKPT ASGAAGMTAA IDAAEAARP SGRTVTATLT PQPARIDLGG PIVSTLTYGN TIPGPLIRAT VGDEIVVSVT NRLGDPTSVH WHGIALRNDM DGTEPATANI GPGGDFTYRF SVPDPGTYWA HPHVGLQGDH GLYLPVVVDD PTEPGHYDAE WIIILDDWTD GIGKSPQQLY GELTDPNKPT MQNTTGMPEG EGVDSNLLGG DGGDIAYPYY LINGRIPVAA TSFKAKPGQR IRIRIINSAA DTAFRIALAG HSMTVTHTDG YPVIPTEVDA LLIGMAERYD VMVTAAGGVF PLVALAEGKN ALARALLSTG AGSPPDPQFR PDELNWRVGT VEMFTAATTA NLGRPEPTHD LPVTLGGTMA KYDWTINGEP YSTTNPLHVR LGQRPTLMFD NTTMMYHPIH LHGHTFQMIK ADGSPGARKD TVIVLPKQKM RAVLVADNPG VWVMHCHNNY HQVAGMATRL DYIL.